Environmental Science and Pollution Research (2020) 27:6723–6748
https://doi.org/10.1007/s11356-019-07469-w

REVIEW ARTICLE

A review of the catalysts used in the reduction of NO by CO for gas purification

Zhicheng Xu[1,2] · Yuran Li[1] · Yuting Lin[1] · Tingyu Zhu[1,3]

Received: 24 September 2019 / Accepted: 18 December 2019 / Published online: 14 January 2020

Abstract

The reduction of NO by the CO produced by incomplete combustion in the flue gas can remove CO and NO simultaneously and economically. However, there are some problems and challenges in the industrial application which limit the application of this process. In this work, noble metal catalysts and transition metal catalysts used in the reduction of NO by CO in recent years are systematically reviewed, emphasizing the research progress on Ir-based catalysts and Cu-based catalysts with prospective applications. The effects of catalyst support, additives, pretreatment methods, and physicochemical properties of catalysts on catalytic activity are summarized. In addition, the effects of atmosphere conditions on the catalytic activity are discussed. Several kinds of reaction mechanisms are proposed for noble metal catalysts and transition metal catalysts. Ir-based catalysts have an excellent activity for NO reduction by CO in the presence of O_2. Cu-based bimetallic catalysts show better catalytic performance in the absence of O_2, in that the adsorption and dissociation of NO can occur on both oxygen vacancies and metal sites. Finally, the potential problems existing in the application of the reduction of NO by CO in industrial flue gas are analyzed and some promising solutions are put forward through this review.

Keywords Noble metal catalysts · Transition metal catalysts · NO reduction · SCR · Carbon monoxide

Introduction

Nitrogen oxides (NO_x) from industrial flue gas are one of the main air pollutants and can cause environmental problems such as photochemical smog, acid rain, and ozone layer depletion. At present, the most mature NO_x emission control technology is ammonia selective catalytic reduction (NH_3-SCR) (Damma et al. 2019). This technology has been widely used in coal-fired power plants. However, ammonia will react with sulfur dioxide (SO_2) and sulfur trioxide (SO_3) in flue gas to form ammonium sulfate, resulting in catalyst deactivation, equipment blockage, and corrosion and may cause secondary pollution due to leakage (Damma et al. 2018). As a reductive atmosphere, carbon monoxide (CO) is commonly found in sintering flue gas, pelletizing flue gas, and coke-oven flue gas. CO is also a colorless, odorless, asphyxiating toxic gas and can lead to human poisoning when the CO content in the air is higher than 0.1%. Using CO instead of NH_3 for denitrification (de-NO_x) can not only reduce the cost of pollution control but also simultaneously eliminate NO_x and CO in the flue gas.

The reduction of NO to N_2 by CO (NO-CO reaction) on a catalyst was studied in the 1950s-1960s (Unland 1973). The idealized NO-CO reaction process is shown in Eq. 1.

$$2CO + 2NO \rightarrow 2CO_2 + N_2 \quad (1)$$

The selective catalytic reduction of NO by CO (CO-SCR) was first proposed by Tauster and Murrelin (S.J.Tauster 1976). The technology of the NO-CO reaction was first applied to motor vehicle exhaust. In recent years, attempts have been made to apply this technology to industrial flue gas.

Responsible editor: Santiago V. Luis

✉ Yuran Li
yrli@ipe.ac.cn

✉ Tingyu Zhu
tyzhu@ipe.ac.cn

[1] Beijing Engineering Research Center of Process Pollution Control, National Engineering Laboratory for Hydrometallurgical Cleaner Production Technology, Institute of Process Engineering, Chinese Academy of Sciences, Beijing 100190, China

[2] University of Chinese Academy of Sciences, Beijing 100049, China

[3] Center for Excellence in Regional Atmospheric Environment, Institute of Urban Environment, Chinese Academy of Sciences, Xiamen 361021, China

However, two major challenges remain in the application of the NO-CO reaction in industry, including oxygen-enriched conditions and a relatively low temperature. To explore catalysts suitable for application in oxygen-enriched and low-temperature conditions, the research progress on catalysts for the NO-CO reaction technology is reviewed, including noble metal catalysts and transition metal catalysts. The effects of the support, additives, pretreatment methods, physicochemical properties of the catalyst, and reaction atmosphere conditions on the catalytic activity were reviewed. The reaction sites, catalytic performance, and reaction mechanism of the NO-CO reaction were summarized and compared. In addition, the challenges and potential of the NO-CO reaction technology in industrial applications are also mentioned. The above contents are expected to provide prospective suggestions for the industrial application of technology for reduction of NO by CO.

Noble metal catalysts

The first catalysts employed for the catalytic reduction of NO by CO were noble metal catalysts. Typical catalysts including Pd-, Pt-, Rh-, Ru-, and Ir-based catalysts are reviewed in the following subsections.

Pd-based catalysts

Pd is a common active component of denitrification catalysts for motor vehicle exhaust (Baidya et al. 2013; Fan and Xiao 2013; Shin et al. 2016; Uchiyama et al. 2015) and has a high temperature tolerance (Gaspar and Dieguez 2000). Researchers have applied Pd-based catalysts to the NO-CO reaction. Among the solid-solution catalysts of Pd, Pt, and Rh doped with CeO_2, the catalytic activity of Pd catalysts was higher than that of Pt and Rh catalysts (Roy and Hegde 2008).

The catalytic activities of Pd are affected by various factors. The support plays an important role in the catalytic activity of the Pd-based catalysts. Loading Pd on CeO_2 or TiO_2 exhibits better NO-CO reaction activity (Roy et al. 2007a; Roy et al. 2007b). Loading Pd on a Ce-Ti solid solution achieves high activity due to the maintenance of the reduced state of Pd (Trovarelli 1997). The Pd-Ni/Al_2O_3 catalyst has the best catalytic activity among Al_2O_3, (Ce, Zr)O_x/Al_2O_3, and (Ce, Zr)O_x supports. In addition, loading Pd on CeO_2 attains higher activity than on Al_2O_3 (Bera et al. 2000).

Additives also affect the catalytic activity of the Pd-based catalysts. Adding VO_x to the Pd/Al_2O_3 catalyst gained a high N_2 selectivity at low temperatures and promoted the dissociation of NO (Neyertz and Volpe 1998). Adding NiO to the Pd/$CeZrO_x$/Al_2O_3 catalyst improved the interaction between Pd and the support and improved the de-NO_x efficiency (Hungria et al. 2005a). After the addition of CeO_2, the activity of the Pd/Al_2O_3 catalyst significantly increased (Ciuparu et al. 2000; Holles et al. 2000). The oxygen vacancies of CeO_2 played an important role in the NO-CO reaction; therefore, the addition of CeO_2 to a catalyst would increase the catalytic activity (Roy and Hegde 2008). With the addition of MoO_x to the Pd/Al_2O_3 catalyst, a high de-NO_x efficiency was obtained due to the formation of Mo^{4+} on the catalyst at low temperature, which lowered the adsorption stability of N atoms on the surface of the Pd and accelerated the dissociation of NO (Noronha et al. 1999). The Cu-doped Pd-based catalysts could effectively activate NO and significantly enhance the dissociation of the N-O bond due to the presence of Cu (Illas et al. 1998). Doping Ba into Pd-based catalysts could reduce the initial conversion temperature of the NO-CO reaction and inhibit the production of N_2O when the temperature is above 200 °C (Tanikawa and Egawa 2011). The addition of the promoter Mo in Pd-based catalysts can improve N_2 selectivity (Schmal et al. 1999).

The physicochemical properties of Pd-based catalysts also influence the catalytic activity. As the particle size of the metallic Pd increases over the Pd/Al_2O_3 catalyst, the NO reduction activity is increased (Fernández-García et al. 2004). The chemical state of Pd depends largely on the size of Pd particles (Iglesias-Juez et al. 2011). When the particle size is 1.5 nm with a Pd loading of 2%, the valence state of Pd is dominated by Pd^+, while the valence state of Pd is dominated by Pd^0 as the particle size increases to 3 nm with a loading of 4%. It can be deduced that the small particles tend to form Pd^+, while Pd^0 is more likely to be formed when the Pd particle is large. It is also reported that Pd^+ has a higher catalytic activity for CO oxidation reaction than Pd^0 in the presence of O_2, while Pd^0 is more conducive to the NO-CO reaction. NO reduction on Pd-based catalysts is not only a structurally sensitive reaction but also dependent on the surface coverage of the gas molecules and the crystal orientation. On the Pd/SiO_2 catalyst, the formation of stable inactive atomic nitrogen species has a significant impact on the NO-CO reaction (Xu et al. 1994). The unstable lattice oxygen plays an important role in the NO-CO reaction over a $Ce_{0.73}Ti_{0.25}Pd_{0.02}O_{2-x}$ catalyst (Baidya et al. 2007).

The mechanism of the NO-CO reaction on the Pd-based catalysts has been proposed by many researchers with the reactions shown in Eqs. 2–6 (Baidya et al. 2007; Chin and Bell 1983; Granger et al. 1998a; Roy et al. 2007a; Roy et al. 2007b).

$$NO_{(ads)} + M \rightarrow N_{(ads)} + O_{(ads)} \quad (2)$$

$$N_{(ads)} + N_{(ads)} \rightarrow N_2 + 2M \quad (3)$$

$$N_{(ads)} + NO_{(ads)} \rightarrow N_2 + O_{(ads)} + M \quad (4)$$

$$N_{(ads)} + NO_{(ads)} \leftrightarrow N_2O + 2M \quad (5)$$

$$O_{(ads)} + CO_{(ads)} \rightarrow CO_2 + 2M \quad (6)$$

M−−Metal sites

Both CO and NO are adsorbed at the Pd site, and the dissociation of NO also occurs at the Pd site. The adsorbed N ($N_{(ads)}$) produced by the dissociation of NO combines with itself to generate N_2, or with another adsorbed NO ($NO_{(ads)}$) to generate N_2 or N_2O. The adsorbed O ($O_{(ads)}$) produced from the dissociation of NO combines with the adsorbed CO ($CO_{(ads)}$) to generate CO_2. In addition, a bifunctional mechanism on the surface of a Pd-MoO_3/Al_2O_3 catalyst was proposed (Noronha et al. 1999): NO is adsorbed and dissociated at the Mn^{4+} site to generate $N_{(ads)}$ and $O_{(ads)}$, and the $O_{(ads)}$ is then transferred to the Pd site, reacting with the $CO_{(ads)}$ on the Pd site and resulting in the formation of CO_2.

The atmospheric conditions can affect the catalytic activity of the catalyst. On Pd/zeolite catalyst, SO_2 can reduce the activity of the NO-CO reaction, and H_2O also reduces catalytic activity due to competitive adsorption among NO, CO, and H_2O (Nakatsuji et al. 2008).

Pt-based catalysts

Pt is a highly active component of the noble metal catalysts for the NO-CO reaction (Granger et al. 1998a). The catalytic activities of Pt are affected by its supports. Higher activity was obtained by loading Pt on CeO_2 than on Al_2O_3 (Bera et al. 2000). Additives can facilitate the Pt-based catalysts. Doping La and Y in the Pd/CeO_2 catalyst can increase the catalytic activity due to the increase in oxygen vacancies where the dissociation of NO can occur (Gayen et al. 2006). On the Pt-Rh bimetallic catalyst, a synergistic effect was found between the two components (Oh and Carpenter 1986).

The mechanism of the NO-CO reaction on the Pt-based catalysts is the same as that on Pd-based catalysts (Araya and Weissmann 2000; Graham et al. 1993; Granger et al. 1998a; Hu et al. 1998); both are the reaction of the $CO_{(ads)}$ and $NO_{(ads)}$ on the catalyst surface. On the Pt/NaX catalyst, N_2 and CO_2 were mainly formed above 230 °C; however, N_2O and CO_2 would be formed below 205 °C (Novakova and Kubelkova 1997). N_2O was speculated as the intermediate of the reaction above 205 °C and continued to participate in the subsequent reaction process to generate N_2. On the Pt/SBA-15 catalyst, the reaction mechanism is that $NO_{(ads)}$ reacts with isocyanate (−NCO) to generate N_2 and CO_2, and the −NCO detected by in situ diffuse reflectance infrared Fourier transform spectra (in situ DRIFT) was considered to be the reaction intermediate (Xiao et al. 2014). The dissociation of the NO can occur at the oxygen vacancies on the Pt/CeO_2 catalyst (Bera et al. 2000).

For the Pt-based catalysts, atmospheric conditions have a significant effect on the NO-CO reaction. The NO-CO reaction is greatly inhibited by the presence of O_2 because of its high CO oxidation activity (Ding et al. 2011; Mergler et al. 1996; Xu et al. 2012). On the Pt/zeolite catalyst, the presence of SO_2 could reduce the activity of the NO-CO reaction since SO_2 was involved in the reaction (Nakatsuji et al. 2008). The NO/CO ratio and O_2 in the atmosphere influenced the N_2 selectivity on the Pt/NaX catalyst. Furthermore, higher NO/CO ratios and O_2 concentrations were beneficial for N_2O formation (Novakova and Kubelkova 1997).

Rh-based catalysts

Rh-based catalysts have also been applied to the NO-CO reaction. Rh-based catalysts have a higher NO dissociation activity compared with Pt and Pd (Shelef and Graham 2006). Different noble metal catalysts were compared, and the order of catalytic activity was found to be Rh > Pd > Pt (Kobylinski and Taylor 1974). Rh/ZSM-5 catalyst has an N_2 selectivity superior to those of Pt/ZSM-5, Pd/ZSM-5, and Ir/ZSM-5 catalysts (Wang et al. 2003). The comparison of Pd, Rh, and Ru catalysts supported on Co_3O_4 showed that the activity order of the NO-CO reaction was $Rh_{0.05}Co_{2.95}O_4 > Pd_{0.05}Co_{2.95}O_4 > Ru_{0.05}Co_{2.95}O_4 > Co_3O_4$ (Salker and Desai 2016). A Rh/SiO_2 catalyst mainly produces N_2O at low temperatures with low N_2 selectivity (Araya et al. 2002). The chemical state of Rh also influences the catalytic activity. On the Rh/SiO_2 catalyst, the Rh in the oxidized state favors catalytic activity better than the Rh in the reduced state (Chin and Bell 1983). On the Rh/zeolite catalyst, Rh^0 is the main active component and Rh^{3+} is the secondary active component (Nakatsuji et al. 2008).

The mechanism of the NO-CO reaction on Rh-based catalysts is the reaction of $CO_{(ads)}$ and $NO_{(ads)}$ on the catalyst surface (Bowker et al. 1993; Goodman et al. 1993; Peden et al. 1988; Schwartz et al. 1986). The mechanism is the same as in Eqs. 2–6 (Chuang et al. 1995; Chuang and Tan 1998; Granger et al. 1998b; Krishnamurthy and Chuang 1995; Krishnamurthy et al. 1995). The rate-determining step of the NO-CO reaction is the dissociation of NO (Oh 1986). N_2O is formed during the NO-CO reaction at low temperatures on Rh/SiO_2 catalyst (Hecker and Bell 1983; Hecker and Bell 1984). An important intermediate reaction between N_2O and CO on the Rh/Al_2O_3 catalyst was found (Cho 1994; K. Cho 1992; Mccabe and Wong 1990). The NO-CO reaction on a Rh/zeolite catalyst is mainly achieved by the formation of −NCO species, which then react with NO to generate N_2 (Nakatsuji et al. 2008). Among Pt, Pd, and Rh catalysts, only the $Ce_{0.98}Pd_{0.02}O_2$ catalyst follows a single-step process, in which the molecular adsorption and dissociation occur on metal ions. In contrast, the $Ce_{0.98}Pt_{0.02}O_2$ and $Ce_{0.98}Rh_{0.02}O_2$ catalysts follow a bifunctional mechanism, in which the molecular adsorption occurs on the metal sites and the dissociation adsorption occurs on the oxygen vacancies, as shown in Eqs. 7–10 (Roy and Hegde 2008). This bifunctional mechanism was also found on Pt/Al_2O_3 and Rh/Al_2O_3 catalysts (Granger et al. 2002).

$$NO + 2\square \leftrightarrow N_{(ads)} + O_{(ads)} \quad (7)$$

$$O_{(ads)} + CO_{(ads)} \rightarrow CO_2 + M^{n+} + \square \quad (8)$$

$$O_{(ads)} + NO_{(ads)} \rightarrow N_2O + M^{n+} + \square \quad (9)$$

$$N_2O + \square \rightarrow N_2 + O_{(ads)} \quad (10)$$

M^{n+}——Metal ions; □——Oxygen vacancy

The atmospheric conditions have a large effect on the catalytic activity of the Rh-based catalysts. CO can promote the oxidation of Rh particles and reduce the catalytic activity below 502 °C (Paul et al. 1990; Paul and Yates 1991). Rich CO conditions can inhibit the de-NO_x efficiency of the Rh-based catalysts, because CO will compete with NO for adsorption sites on the catalyst surface (Haneda et al. 2005; Haneda et al. 2003). However, the presence of SO_2 can improve the activity of the NO-CO reaction on Rh/Na-β zeolite catalyst.

Ru-based catalysts

Ru-based catalysts are excellent heterogeneous catalysts (Yin et al. 2004), with a higher catalytic activity for the NO-CO reaction in noble metal catalysts (Kobylinski and Taylor 1974; Muraki and Fujitani 1986). On the same support, Ru-based catalysts can achieve higher catalytic activity than the other metal catalysts. For a series of catalysts supported by MCM-41 through the coprecipitation method, the activity decreases in the following order when the temperature is below 277 °C: Ru/MCM-41 > Co/MCM-41 > Ni/MCM-41 ≈ Fe/MCM-41 ≈ Cu/MCM-41. When the temperature is above 377 °C, Ru/MCM-41 still has a higher catalytic activity, second only to Cu/MCM-41 (Patel et al. 2014). On a perovskite support, the activity of the active components decreased in the order of Cu-Ru > Ni-Ru > Cu-Ti > Ni-Ti (Teraoka et al. 2000).

The support has an effect on the catalytic activity of the Ru-based catalysts. The Ru/mordenite catalyst has a larger specific surface area, active component dispersity, and ion exchange performance than other catalysts with different supports (Labhsetwar et al. 2007). The strong interaction between Ru and the carrier $La_{1.6}Ba_{0.4}NiO_4$ (LBN) occurred in Ru/LBN catalyst causing high catalytic activity. This strong interaction enhanced the reducibility of the catalyst and the mobility of the oxygen species, thus increasing the $CO_{(ads)}$ and $NO_{(ads)}$ contents on the catalyst surface. Ru has higher stability on hexa-aluminate, which greatly enhances its catalytic activity (Zhang et al. 2013). Additives have a promoting effect on the catalytic activity of the Ru-based catalysts. Doping Cu in a Ru/SiO_2 catalyst can strongly avoid the poisoning of Ru (López et al. 1999).

The physicochemical properties of the Ru-based catalysts also have an obvious effect on the catalytic activity. The catalytic activity of Ru-based catalysts is closely related to particle morphology, active component dispersion, and degree of agglomeration. The Ru nanoparticles with a size of 1–3 nm and a high dispersion of 70% have a higher catalytic activity and greater stabilization than those with a size of 10–80 nm and a low dispersion of 10% (Komvokis et al. 2011). A good dispersion of Ru particles obtained on $Ru/Mg_xAl_yO_z$ catalyst results in excellent NO storage capacity (Li et al. 2007). CO pretreatment can also enhance the catalytic activity of Ru-based catalysts (Iliopoulou et al. 2005a).

The reaction mechanism of the NO-CO reaction on Ru-based catalysts has been proposed. On a Ru/perovskite catalyst, some highly reactive adsorbed species such as inorganic carboxylate, monodentate carbonate, Ru-NO, bridged nitrate (NO_3^-), and nitrite (NO_2^-) are found in the NO-CO reaction, as detected by in situ DRIFT. Ru^{3+} is found to be the main active site (Sui et al. 2017). On a Ru/zeolite catalyst, CO is adsorbed on Ru^{3+} in the form of a dimer to form Ru^{3+}-$(CO)_2$, and NO is adsorbed on Ru^{2+} to form Ru^{2+}-NO^+ (Lei and Kevan 1991). On $La_{0.8}Sr_{0.2}Al_{1-2y}Cu_yRu_yO_3$ catalyst, the CO oxidation and NO-CO reaction are achieved by a redox cycle, in which Cu and Ru act in two respective processes, with the mechanism shown in Fig. 1 (Teraoka et al. 2000).

Atmospheric conditions have a large influence on the Ru-based catalysts. O_2-rich conditions can suppress the NO-CO reaction and the de-NO_x efficiency on Ru-based catalysts (Teraoka et al. 2000). Furthermore, the Ru-based catalysts are sintered at a lower temperature of approximately 400 °C in the presence of O_2 (Koopman et al. 1981; López et al. 1999). Ru will form a series of oxides (RuO_3, RuO_4) with lower sublimation temperature (Taylor 1974), which will easily sinter in the presence of O_2 (López et al. 1999). The H_2O in the atmosphere also exerts an inhibitory effect on the Ru-based catalysts (Li et al. 2012). NH_3 formation was found on Ru/Al_2O_3 catalysts at low temperatures of 200–400 °C under an atmosphere of NO+CO + H_2 + H_2O + CO_2 + He. N_2O is an intermediate product formed in the reaction between CO and NO (Voorhoeve and Trimble 1975). However, Ru-based catalysts have better sulfur resistance than Pt-, Pd-, and Rh-based catalysts (Hornung et al. 1998). The

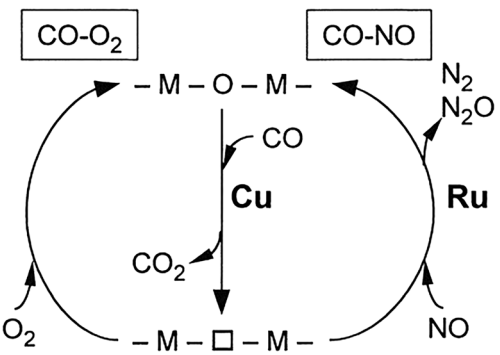

Fig. 1 Mechanism of CO oxidation and the NO-CO reaction on $La_{0.8}Sr_{0.2}Al_{1-2y}Cu_yRu_yO_3$ catalyst (Teraoka et al. 2000). Copyright 2000, Elsevier

SO_2 in the atmosphere has a slight influence on Ru-based catalysts. In addition to the influence of the atmosphere, metal loss from and the toxicity of Ru-based catalysts have become another obstacle to their industrial application.

Ir-based catalysts

The noble metal Ir has been extensively studied in the field of the NO-CO reaction due to its excellent antioxidant properties. Ir-based catalysts have the highest catalytic activity among the Pd-, Rh-, Pt-, and Ir-based catalysts supported on ZSM-5 (Wang et al. 2003). This conclusion has been recognized by other researchers (Haneda et al. 2005; Haneda et al. 2003; Inomata et al. 2007; S.J.Tauster 1976; Shimokawabe et al. 2005).

The support can influence the catalytic activity of the Ir-based catalysts. Ir/silicalite has better performance than Ir/SiO_2 and Ir/Al_2O_3 (Ogura et al. 2000); moreover, Ir/WO_3 is superior to Ir/ZnO (Shimokawabe et al. 2005). Additives also have a large effect on the catalytic activity of Ir-based catalysts. Adding Nb_2O_5 to the Ir/SiO_2 catalyst increased the stability of the catalyst because the Nb_2O_5 further enhanced the oxidation-resistance capacity of the Ir on the catalyst surface (Tamai et al. 2007). When the content ratio of the additive to the Ir was 1:10, the doping of Li, Na, K, Mg, Sr, Ba, W, Mo, Co, Zn, Au, and Ru on the Ir/SiO_2 catalyst has a positive effect on the catalytic activity in the presence of O_2, SO_2, and H_2O. The promoting effect of Ba was the most obvious (Haneda et al. 2006b). The promotion of alkaline earth metals is attributed to the inhibition of the oxidation of Ir to IrO_2 (Haneda et al. 2006b).

Pretreatment can influence the catalytic activity of the catalyst. Activation of Ir-based catalysts involves high-temperature pretreatment (Nawdali et al. 2001a; Nawdali et al. 2001b; Wang et al. 2001) and in situ activation during catalytic experiments (Iojoiu et al. 2004; Wögerbauer et al. 2001b), both of which result in crystal growth and the coexistence of Ir and IrO_2 (Wögerbauer et al. 2001b; Wögerbauer et al. 2001c). Dendrimer–metal nanocomposites (DMNs) were used as precursors to prepare dendritic Ir-Au catalysts, which exhibit a higher dispersion than conventional catalysts, resulting in a higher catalytic activity (Song et al. 2014; Song et al. 2013). When the pretreatments of Ir/WO_3/TiO_2 catalyst were compared, the catalytic activity of the catalyst treated with H_2O, $H_2O + CO$ or $H_2O + O_2 + CO$ was enhanced approximately 1.5–2 times relative to the activity without pretreatment (Takahashi et al. 2006). The reason was that after H_2O treatment, the strong interaction species formed between Ir and WO_3 on the catalyst surface, which was the active center of the NO-CO reaction. The Ir-based catalysts after reduction pretreatment exhibited superior performance in the NO-CO reaction compared with the catalysts after oxidation pretreatment (Haneda et al. 2005). The NO conversion efficiency on 10%Nb_2O_5/Ir/SiO_2 catalyst was 80%, significantly higher than the value of 30% on Ir/10%Nb_2O_5/SiO_2 catalyst (Tamai et al. 2007). The interaction between Nb_2O_5 and Ir makes Ir difficult to oxidize, thus promoting the activity of the catalyst (Tamai et al. 2007).

The activity of the catalyst is also related to the physicochemical properties. The size of the Ir particles has an important effect on the de-NO_x activity (Iojoiu et al. 2004; Wögerbauer et al. 2001a; Wögerbauer et al. 2001b; Wögerbauer et al. 2001c). Better dispersion is obtained when the Ir particle size is smaller than 2 nm. Moreover, the size of the Ir particles is related to the competition between the NO-CO reaction and CO oxidation (Fan and Xiao 2013; Iliopoulou et al. 2004; Uchiyama et al. 2015). On the Ir/SiO_2 catalyst, with different Ir dispersions ranging from 86 to 6%, the NO-CO reaction activity is strongly dependent on the Ir dispersion in the presence of O_2 and SO_2 with the maximum activity being attained at 10–20% (Haneda et al. 2006a). On the Ir-Au/Al_2O_3 catalyst, the NO-CO reaction and the dissociation of NO are structure-sensitive reactions (Song et al. 2014). The size effect and structural sensitivity of Ir-based catalysts have also been demonstrated by other researchers through infrared spectroscopy analysis (Chen et al. 2010b). Therefore, the preparation processes of the Ir-based catalysts must control the size of the Ir particles, the dispersion of Ir, and the structure of the catalyst to achieve a better performance.

The reaction mechanism of Ir-based catalysts is different from that of Pd-, Rh-, and Pt-based catalysts. The active center of Ir-based catalysts is Ir^0 (Haneda et al. 2005). The reaction between $NO_{(ads)}$ and $CO_{(ads)}$ occurs on the same Ir site (Haneda et al. 2005), as shown in Eqs. 11–15.

$$NO + CO + Ir \leftrightarrow Ir_{-NO}^{-CO} \quad (11)$$

$$Ir_{-NO}^{-CO} \rightarrow Ir_{-N} + CO_2 \quad (12)$$

$$Ir_{-N} + Ir_{-N} \rightarrow 2Ir + N_2 \quad (13)$$

$$Ir_{-N} + NO \rightarrow Ir_{-NNO} \rightarrow Ir + N_2O \quad (14)$$

$$Ir_{-N} + CO \rightarrow Ir_{-NCO} \quad (15)$$

The atmospheric conditions will affect the catalytic activity of the NO-CO reaction on Ir-based catalysts. When noble metal catalysts are used, CO is easily consumed by oxidation and the dissociation of O_2 predominates in the presence of excess O_2, blocking the active site of the NO dissociation. Therefore, the presence of excess O_2 inhibits the dissociation of NO and further reduces or even inhibits the de-NO_x efficiency. Tauster et al. (S.J.Tauster 1976) suggest that Ir is the only noble metal active component suitable for the NO-CO reaction under rich O_2 conditions. Among the Ir-, Rh-, Pt-, and Pd-based catalysts supported on Al_2O_3, Ir has a greater ability to dissociate NO in the presence of O_2 than the other noble metals (Taylor and Schlatter 1980). This is because the NO is

more easily adsorbed on the surface of the Ir-based catalysts than O_2, thus ensuring the activity of the NO-CO reaction (S.J.Tauster 1976). On the Rh-based catalysts, excessive CO in the atmosphere will compete with NO for adsorption, while there are two NO adsorption sites on Ir with both top and concave sites. The concave site only adsorbs NO, ensuring the adsorption of NO on the catalyst surface (Haneda et al. 2005; Haneda et al. 2003). The SO_2 (Haneda et al. 2006b; Haneda et al. 2005; Haneda et al. 2003; Inomata et al. 2007; Ogura et al. 2000; Shimokawabe et al. 2005; Yoshinari et al. 2001; Yoshinari et al. 2003) and H_2O (Haneda and Hamada 2008; Haneda and Hamada 2010) in the gas phase have a promoting effect on the NO-CO reaction on the Ir-based catalysts. The promotion effect of SO_2 is attributed to the disproportionation of SO_2 on the Ir surface, and elemental S is present on the catalyst surface (Fujitani et al. 2007). As shown in Eqs. 16–17, the S reacts with surface oxygen and oxidized Ir to maintain the reduced state of the active site Ir^0. H_2O is not directly involved in the reaction (Haneda and Hamada 2008; Haneda and Hamada 2010). The promotion by H_2O is attributed to the in situ hydrogen production through the water gas shift reaction, which maintains the reduced state of Ir, thus ensuring the activity of the catalyst.

$$3SO_{2(ads)} \rightarrow 2SO_{3(ads)} + S_{(ads)} \quad (16)$$

$$S_{(ads)} + 2O_{(ads)} \rightarrow SO_2 \quad (17)$$

Summary

A great deal of research on noble metal Pd-, Pt-, Rh-, Ru-, and Ir-based catalysts has been conducted. Performances of the partial noble metal catalysts for the NO-CO reaction are summarized in Table 1. It is concluded that the mechanism of the NO-CO reaction on these catalysts is basically similar in that both CO and NO are first adsorbed on the catalyst surface and the reaction then follows the Langmuir-Hinshelwood (L-H) mechanism. The difference is that CO and NO are adsorbed at two active sites on the Pd-, Pt-, Rh-, and Ru-based catalysts, as shown in Fig. 2a, while CO and NO are adsorbed at one active site on the Ir-based catalysts, as shown in Fig. 2b. After adsorption, the dissociation of NO which determines the rate of the NO-CO reaction comes into play. Subsequently, $N_{(ads)}$ and $O_{(ads)}$ produced by the dissociation of NO combined with CO, NO, or themselves to generate a number of products, byproducts, and reaction intermediates such as N_2, CO_2, N_2O, and −NCO. The key to improving the catalytic activity is to promote the dissociation of NO.

*N-O bond dissociation rate in $N_2O_{(ads)}$ is lower than $N_2O_{(ads)}$ desorption rate

#N-O bond dissociation rate in $N_2O_{(ads)}$ is higher than $N_2O_{(ads)}$ desorption rate

The NO-CO reaction on noble metal catalysts is seriously affected by atmosphere. Based on the actual conditions of industrial flue gas, the effect of various flue gas components on the catalytic activity of the noble metal catalysts is shown in Table 2. The catalytic activity of the Pd-, Pt-, and Ru-based catalysts is strongly suppressed by SO_2, H_2O, and O_2. On the Rh-based catalysts, the catalytic activity is promoted by SO_2, but obviously inhibited by H_2O and O_2. On the Ir-based catalysts, SO_2 and H_2O significantly promote the NO-CO reaction activity, while O_2 exhibits a little negative effect. At present, the Ir-based catalysts are the most active noble metal catalysts for the NO-CO reaction under actual industrial flue gas conditions among all the noble metal-based catalysts. SiO_2, WO_3, Nb_2O_5, and Ta_2O_5 are good supports for Ir-based catalysts; Ba and Sr are excellent promoters. The reduced state of Ir is an important prerequisite to ensure the high activity of Ir-based catalysts in the NO-CO reaction. Ir-based catalysts exhibit excellent properties such as low-temperature activity, N_2 selectivity, O_2 resistance, H_2O resistance, and sulfur resistance. However, they suffer some drawbacks, such as their high cost and the narrow temperature range of the catalytic reaction. Therefore, the widespread application of Ir-based catalysts in industrial flue gas is limited, and further research is urgently needed.

Transition metal catalysts

Noble metals have the disadvantages of high price, harmful to the environment, and high temperature required for their use. Therefore, in the past decade, researchers have begun to study a large number of transition metal catalysts to catalyze the NO-CO reaction. Typical catalysts such as Cu-, Fe-, Co-, Mn-, and Ni-based are reviewed in the following subsections. Mono-metallic catalysts and bimetallic catalysts are discussed respectively.

Cu-based mono-metallic catalysts

Thirty years ago, Iwamoto et al. (Iwamoto et al. 1989; Iwamoto et al. 1990) first found that the Cu/ZSM-5 catalyst has a good ability to dissociate NO. Afterwards, the researchers conducted a large amount of experimental research on the NO-CO reaction using Cu-based catalysts.

Supports will influence the catalytic activities. Cu^{2+} on the CeO_2 support is more active than Cu^{2+} without support (Bera et al. 2002). The catalytic activities of CuO catalyst and crystalline CuO with different supports were studied, and the order of activity was found to be $CuO/CeO_2 > CuO/\gamma\text{-}Al_2O_3 >$ crystalline CuO (Hu et al. 2001). When CuO catalyst was loaded on Al_2O_3 and ZrO_2 supports, the activity decreased in the order $CuO/ZrO_2\text{–}Al_2O_3 > CuO/ZrO_2/Al_2O_3 > CuO/Al_2O_3$ (Yu et al. 2012). As Cu-based catalysts

Table 1 Activity of various noble metal catalysts for the NO-CO reaction

Catalyst	Reaction conditions						T_{20}[c] (°C)	T_{50}[d] (°C)	T_{max}[e] (°C)	NO conversion (%)	N_2 selection (%)	References
	Temperature range (°C)	GHSV[a] or WHSV[b]	NO (ppm)	CO (ppm)	O_2 (%)	Other gases						
$Ru/La_{1.6}Ba_{0.4}NiO_4$	300–500	0.12 g s cm^{-3}	5000	5000	\	\	325	340	500	100	95	(Sui et al. 2017)
Pd-Au/TiO_2	120–450	3.18 g s cm^{-3}	10,000	10,000	\	\	150	189	350	100	60	(Shin et al. 2016)
Pd/TiO_2	120–450	3.18 g s cm^{-3}	10,000	10,000	\	\	170	205	350	100	64	(Shin et al. 2016)
Au/TiO_2	120–450	3.18 g s cm^{-3}	10,000	10,000	\	\	185	258	350	100	64	(Shin et al. 2016)
Ru-MCM-41	150–450	0.075 g s cm^{-3}	250	750		\	200	237	250	100	\	(Ohyama et al. 2016)
$Rh_{0.05}Co_{2.95}O_4$	100–400	0.576 g s cm^{-3}	50,000	50,000	\	\	180	225	300	100	100	(Salker and Desai 2016)
Pd/$LaSrMnO_4$	110–450	37,500 h^{-1}	5420	5160	\	\	250	310	350	100	80	(Uchiyama et al. 2015)
Ir-Au/Al_2O_3	25–600	10,000 ml g^{-1} h^{-1}	2000	2000	\	\	250	280	350	95	\	(Song et al. 2014)
Pt/SBA-15	320–500	0.024 g s cm^{-3}	4000	4000	\	\	340	360	420	100	\	(Xiao et al. 2014)
2%Pd/Al_2O_3	150–350	0.002 g s cm^{-3}	5000	5000	\	\	200	250	275	100	50	(Baidya et al. 2013)
$Ce_{0.98}Pd_{0.02}O_{2-x}$	110–350	0.002 g s cm^{-3}	5000	5000	\	\	130	150	275	100	45	(Baidya et al. 2013)
$Ce_{0.73}Sn_{0.25}Pd_{0.02}O_{2-x}$	75–300	0.002 g s cm^{-3}	5000	5000		\	100	115	145	100	20	(Baidya et al. 2013)
Ir/WO_3/SiO_2	225–600	75,000 h^{-1}	500	3000	5	1 ppm SO_2、6% H_2O	220	250	280	78	\	(Haneda and Hamada 2010)
Ir/WO_3/SiO_2	225–600	75,000 h^{-1}	500	3000	5	1 ppm SO_2、10% H_2O	240	260	290	80	\	(Haneda and Hamada 2008)
2%Rh/Zeolite	250–400	50,000 h^{-1}	500	15,000	9	6% H_2O、0.5% H_2	\	\	350	55.8	92.2	(Nakatsuji et al. 2008)
Ir/WO_3	300	60,000 h^{-1}	5000	20,000	3	100 ppm SO_2	\	\	300	81	62	(Inomata et al. 2007)
3%Ru-Mordenite	150–400	3900 h^{-1}	1000	1000		\	190	220	400	100	\	(Labhsetwar et al. 2007)
Ba/Ir/SiO_2	240–500	75,000 h^{-1}	500	3000	5	1 ppm SO_2、6% H_2O	\		300	64	87	(Haneda et al. 2006b)
Sr/Ir/SiO_2	240–500	75,000 h^{-1}	500	3000	5	1 ppm SO_2、6% H_2O	\	\	300	55	83	(Haneda et al. 2006b)
5%Ir/WO_3	300–400	0.06 g s cm^{-3}	1000	10,000	2	100 ppm SO_2	\	\	300	83	49	(Shimokawabe et al. 2005)
Pd-Ni/Al_2O_3	27–377	30,000 h^{-1}	1000	10,000	0.45	\	\	147	187	100	\	(Hungria et al. 2005b)
Pd/$Ce_{0.6}Zr_{0.4}O_2$	50–400	0.068 mg s cm^{-3}	230	680	10.5	\	\	200	400	70	84	(Chen et al. 2005)
Pd/Al_2O_3	20–550	30,000 h^{-1}	1000	10,000	0.9	1000 ppm C_3H_6	460	510	\	\	\	(Fernández-García et al. 2004)
Pd/$Ce_{0.5}Zr_{0.5}O_2$/Al_2O_3	20–550	30,000 h^{-1}	1000	10,000	0.9	1000 ppm C_3H_6	525	545	\	\	\	(Fernández-García et al. 2004)
1%Pd/Al_2O_3	27–377	30,000 h^{-1}	1000	10,000	0.45	\	\	147	177	100	98	(Martínez-Arias et al. 2004)
5%Ir/SiO_2	300–500	75,000 h^{-1}	1000	6000	5	20 ppm SO_2、6% H_2O	\		350	51	88	(Haneda et al. 2003)
5%Ir/Al_2O_3	350–500	75,000 h^{-1}	1000	6000	5	20 ppm SO_2、6% H_2O	\		400	17	89	(Haneda et al. 2003)
Ir/SiO_2	300–600	75,000 h^{-1}	1000	3000	0.65	20 ppm SO_2、10% H_2O	300	\	400	58	84	(Yoshinari et al. 2003)
0.02%Ir/Al_2O_3	300–500	40,000 h^{-1}	1000	7500	1	\	370	\	400	45	\	(Ogura et al. 2000)
0.02%Ir/Silicalite	300–500	40,000 h^{-1}	1000	7500	1	150 ppm SO_2	300	330	405	58	\	(Ogura et al. 2000)
0.02%Ir/Silicalite	300–500	40,000 h^{-1}	1000	7500	10	150 ppm SO_2	320	\	360	45	\	(Ogura et al. 2000)
0.02%Ir/SiO_2	300–500	40,000 h^{-1}	1000	7500	1	\	340	360	380	80	\	(Ogura et al. 2000)
Rh/Al_2O_3	200–500	86,000 h^{-1}	400	400	\		200	230	300	100	95	(Cho 1994)
Ru/Al_2O_3	150–500	18,000 h^{-1}	1300	30,000	\	3% H_2O、3% CO_2、0.4% H_2	170	300	480	100	\	(Voorhoeve and Trimble 1975)

[a] GHSV means gaseous hourly space velocity (h^{-1})

[b] WHSV means weight hourly space velocity (g s cm^{-3})

[c] T_{20} represents the temperature when the efficiency is 20%

[d] T_{50} represents the temperature when the efficiency is 50%

[e] T_{max} represents the temperature when the efficiency is maximum

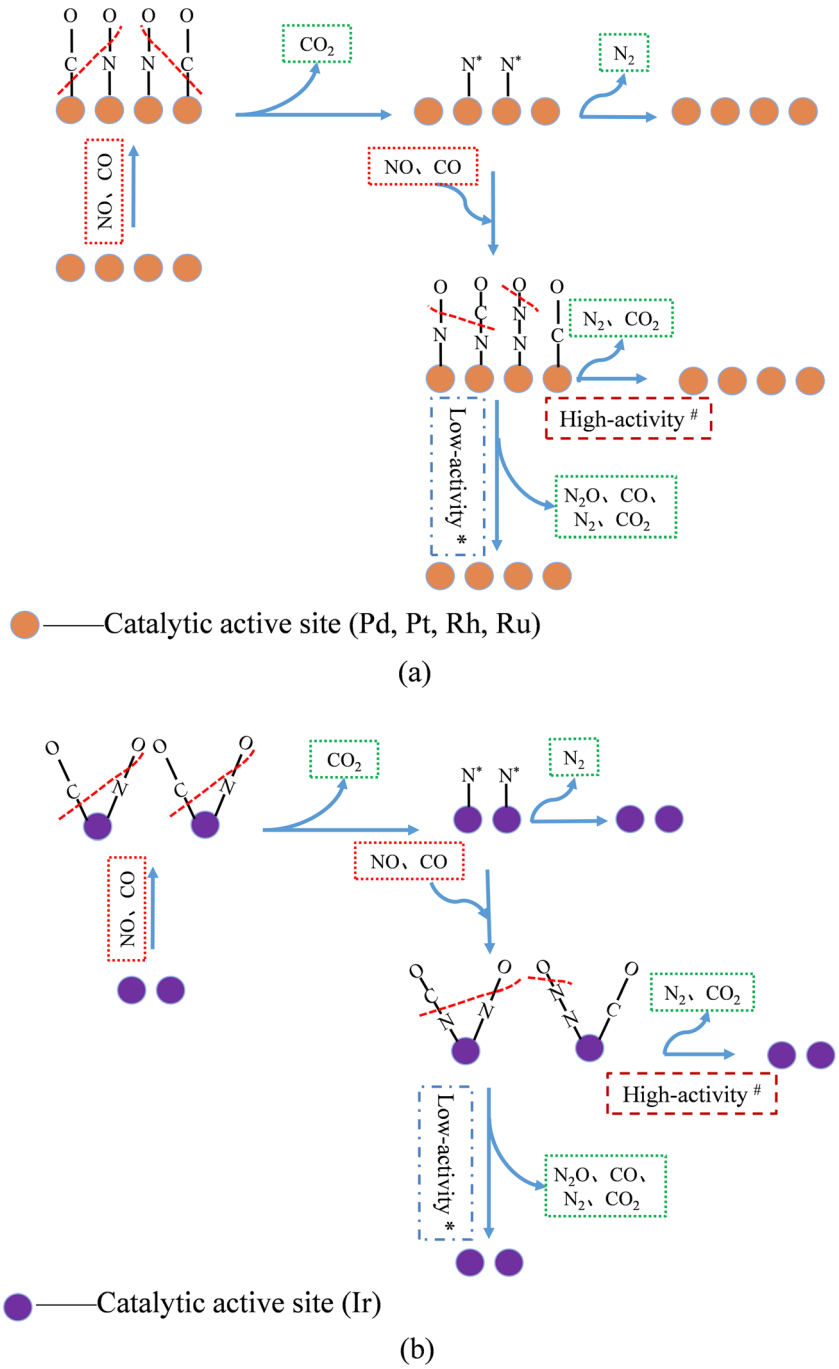

Fig. 2 The mechanism of the NO-CO reaction on Pd-, Pt-, Rh-, Ru-based catalysts (**a**) and Ir-based catalysts (**b**)

were loaded on SBA-15, MCM-41, MCM-48, and KIT-6 supports, CuO/MCM-41 and CuO/SBA-15 showed higher catalytic activity, due to the greater amounts of reductive Cu obtained on MCM-41 and SBA-15 (Patel et al. 2011).

Doping aids the Cu-based catalysts and will increase the catalytic activity. The addition of V to the Cu-based catalysts facilitates the dispersion of CuO and enhances the catalytic activity. Moreover, the addition of Fe, Co, Mn, and Ni generates more oxygen vacancies and improves the mobility of the reactive cations (Zhang et al. 2007b). Addition of ZrO_2 to CuO/TiO_2 catalyst shifted the dissociation peak of NO to a lower temperature in temperature-programmed desorption (TPD), indicating that the catalytic activity toward dissociation of NO was improved (Jiang et al. 2004). The addition of ZrO_2 to CuO/Al_2O_3 catalyst benefited the dispersion of CuO and obtained higher activity (Yu et al. 2012).

Pretreatment can increase the catalytic activity of Cu-based catalysts. The redox treatment of $Cu/MgO\text{-}CeO_2$ catalyst can

Table 2 Effect of flue gas components on the catalytic activity of noble metals

Catalysts	SO_2	H_2O	O_2
Pd-based	↓↓	↓	↓↓
Pt-based	↓↓	↓	↓↓
Ru-based	↓	↓	↓↓
Rh-based	↑	↓	↓↓
Ir-based	↑↑	↑	↓

↓means negative effect;↑means positive effect

further promote Cu to occupy the crystal lattice of Ce and generate a Cu-O-Ce solid solution, thus obtaining higher activity (Chen et al. 2009a). CO pretreatment also promotes the NO-CO reaction activity of the catalyst (Gu et al. 2014; Xiong et al. 2014).

Physicochemical properties also affect the NO-CO reaction activity. On the $CuO/Ce_{0.8}Zr_{0.2}O_2$ catalyst, the catalytic activity and N_2 selectivity are closely related to the loading and particle size but are independent of the dispersion of CuO (Ma et al. 2003). However, the activity on CuO/CeO_2 catalyst was affected by the dispersion of CuO, but not on the size of the CuO particles (Hu et al. 2001).

Various reaction mechanisms on Cu-based catalysts for the NO-CO reaction have been proposed. On $Cu/\gamma\text{-}Al_2O_3$ catalyst, CO is adsorbed at the Cu^+ site and NO is adsorbed at the Cu^{2+} site (Fu et al. 1991). However, other researchers proposed that CO is adsorbed at both the Cu^+ and Cu^{2+} sites, NO is adsorbed at Cu^{2+} site, and the NO dissociation occurs on the Cu^+ site (Zhang et al. 2018c). On Cu-based catalyst supported on benzene-1,3,5-tricarboxylate (BTC), CO is easily adsorbed on Cu^+ to form $Cu^+(CO)_n$ ($n = 1$–4), and NO is also adsorbed on Cu^+ to form $Cu^+(NO)_n$ ($n = 1$–2); Cu^+ is the main site of the NO-CO reaction, and the NO-CO reaction follows the L-H mechanism (Qin et al. 2016). The mechanism of the NO-CO reaction is shown in Eqs. 18–23. The reaction mechanism for the NO-CO reaction on noble metal catalysts (Boccuzzi et al. 1994; Okamoto and Gotoh 1997; Shelef and Graham 2006) is also considered applicable to Cu-based catalysts (Jiang et al. 2004).

$$CO + Cu^+ \leftrightarrow CO_{(ads)} \quad (18)$$

$$NO + Cu^+ \leftrightarrow NO_{(ads)} + Cu^{2+} \quad (19)$$

$$NO_{(ads)} + Cu^+ \rightarrow N_{(ads)} + O_{(ads)} + Cu^{2+} \quad (20)$$

$$CO_{(ads)} + O_{(ads)} \rightarrow CO_2 \quad (21)$$

$$N_{(ads)} + N_{(ads)} \rightarrow N_2 \quad (22)$$

$$\square + Cu^{2+} \rightarrow Cu^+ \quad (23)$$

□—oxygen vacancy;

Some researchers reported that the path of the NO-CO reaction on Cu-based mono-metallic catalysts is different at various temperatures. For the $CuO/Ce_{20}Sn_1O_x$ catalyst, at 25–50 °C, NO was adsorbed on the catalyst surface, and NO_3^- and NO_2^- species were formed inhibiting CO adsorption as shown in Fig. 3. At 50–125 °C, some $NO_{(ads)}$ was released and CO was adsorbed without the redox reaction between CO and Cu^{2+}. Furthermore, the gaseous CO molecules can react with the adsorbed NO species through the Eley–Rideal (E–R) mechanism to produce small amounts of N_2O, N_2, and CO_2 below 150 °C. When the temperature was increased to 150 °C, synergistic interactions of Eqs. 24 and 25 occurred; these interactions generated more Ce^{3+} sites and oxygen vacancies, thereby benefiting CO adsorption and NO desorption, and then generated more N_2, N_2O, and CO_2. At the same time, CO reduced some Cu^{2+} to Cu^+ as shown in Eq. 26. Above 275 °C, CO reduced Cu^+ to Cu^0, with the latter potentially enhancing the transformation of N_2O to N_2 (Deng et al. 2016).

$$Sn^{2+} + 2Ce^{4+} \rightarrow Sn^{4+} + 2Ce^{3+} \quad (24)$$

$$Cu^{2+} + Ce^{3+} \rightarrow Cu^+ + Ce^{4+} \quad (25)$$

$$CO + Cu^{2+} \rightarrow CO_2 + Cu^+ \quad (26)$$

In addition, oxygen vacancies also play an important role in Cu-based mono-metallic catalysts. When the molar ratio of Ti:Ce is 60:1 on the $CuO/TiO_2\text{-}CeO_2$ catalyst, there are more oxygen vacancies and greater mobility of surface oxygen and lattice oxygen (Deng et al. 2015), both of which are related to the reducibility of the catalyst and the regeneration of oxygen vacancies. Oxygen vacancies act as adsorption and dissociation sites of NO, and the Cu^+ site acts as the adsorption site for CO. High catalytic activity and N_2 selectivity were obtained due to the high Cu^+ content and strong synergistic effect between Ti^{3+}, Ce^{3+}, and Cu^+.

On Cu-based catalysts, the dissociation of NO is generally believed to be the rate-determining step for the NO-CO reaction (Boningari et al. 2018; Chen et al. 2013; He et al. 2007; Iglesias-Juez et al. 2004; Jiang et al. 2004; Makeev and Peskov 2013; Rasko 1981; Solymosi and Bansagi 1995; Sun et al. 2009; Wang et al. 2003; Yu et al. 2012). Cu^+ is the activation site for NO (Guerrero et al. 2012). CO can be efficiently adsorbed on Cu^+ site (Martínez-Arias et al. 2012; Senanayake et al. 2016), and competitive adsorption occurs between NO and CO on Cu^+ sites (Hungria et al. 2005b; Xiong et al. 2014). CO reduction treatment can enhance the activity of the Cu-based catalysts because of the pre-adsorption of CO and the formation of Cu^+ (Gu et al. 2014; Xiong et al. 2014).

Non-Cu-based mono-metallic catalysts

In addition to Cu-based catalysts, other transition metal components have also been used for research on the NO-CO reaction due to their similar electronic properties and redox properties. On the Cr/activated carbon (AC) catalyst, the oxygen-

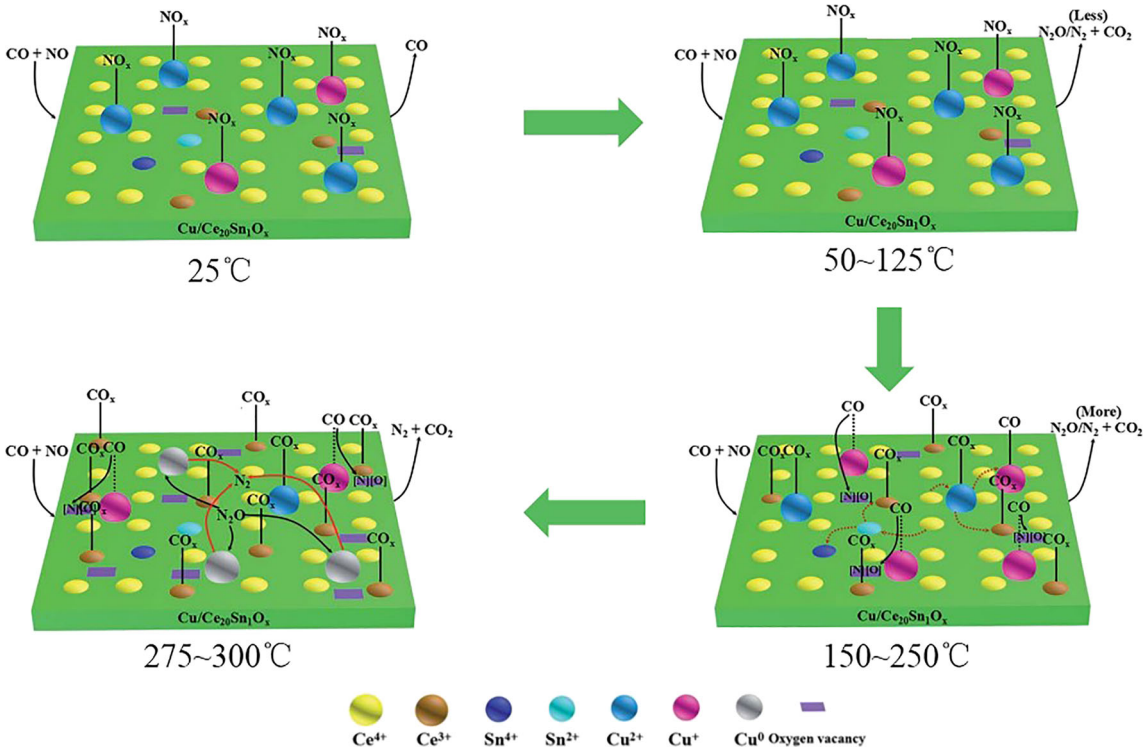

Fig. 3 The mechanism of the NO-CO reaction on $CuO/Ce_{20}Sn_1O_x$ catalyst (Deng et al. 2016) Copyright 2016, Royal Society of Chemistry

containing functional groups on the AC surface play an important role in the reduction of NO and the dispersion of Cr (Rosas et al. 2010; Rosas et al. 2012). By comparing the heat treatment of Cr/AC, it is found that C-O functional groups play an important role in the reduction of NO, which is consistent with the results of other studies (Grzybek et al. 2004; Li et al. 1998; Li et al. 1999; Szymański et al. 2004). In addition, O_2 may produce oxygen-containing functional groups to promote the de-NO_x efficiency. Co species have the ability to dissociate NO (Simonot et al. 1997). On Co/AC catalyst in the absence of O_2, the products were mainly N_2O; the N_2 selectivity was lower when the temperature was below 300 °C (Mehandjiev and Bekyarova 1994). N_2O is proposed as an intermediate of the NO-CO reaction and cannot be further converted to N_2 due to its low activity at low temperature. On TiO_2-promoted cobalt sulfide catalyst, the mechanism is shown in Eqs. 27–32 (Zhang and Yang 2003), in which sulfur vacancy exhibits a role similar to that of oxygen vacancy.

$$S^* + 2NO_{(ads)} \rightarrow 2N_{(ads)} + 2O_{(ads)} \quad (27)$$

$$N_{(ads)} + N_{(ads)} \rightarrow N_2 \quad (28)$$

$$NO_{(ads)} + N_{(ads)} \rightarrow N_2O \quad (29)$$

$$S^* + 2NO_{(ads)} \rightarrow N_2O + O_{(ads)} \quad (30)$$

$$CO_{(ads)} + O_{(ads)} \rightarrow CO_2 \quad (31)$$

$$S^{\#} + 2O_{(ads)} \rightarrow SO_2 \quad (32)$$

S^*—Sulfur vacancy; $S^{\#}$—Sulfide ion in the lattice

Mn-based catalysts have also been extensively studied. In the presence of O_2, the MnO_x/TiO_2 catalyst has a high N_2 selectivity for the NO-CO reaction at 200 °C. When the O_2 concentration increases from 0 to 4 vol%, the activity of the catalyst increases monotonically, accompanied by the stepwise reduction of the oxidation state of Mn on the catalyst surface (Sreekanth and Smirniotis 2007). The NO-CO reaction activity of various transition metal oxide catalysts supported on Al_2O_3 and ZrO_2 was investigated. With a loading of 10 wt%, the activity decreases in the order Fe_2O_3>$CuCr_2O_4$>Cu_2O>Cr_2O_3>NiO>Co_3O_4>MnO>V_2O_5.

Cu-based bimetallic catalysts

With continuing research, the researchers have found that oxygen vacancies play an important role in the NO-CO reaction (Bellido and Assaf 2009; Boaro et al. 2004; Boningari et al. 2018; Chen et al. 2010a; Chen et al. 2009b; Chen et al. 2013; Cheng et al. 2018; Dong et al. 2014; Dong et al. 2011; Gholami and Luo 2018; Gu et al. 2014; He et al. 2007; Huang et al. 2000; Kacimi et al. 2015; Li et al. 2011a; Li et al. 2013; Lv et al. 2013; Makeev and Peskov 2013; Oh et al. 1986; Song et al. 2007; Wang et al. 2017a; Wang et al. 2017c; Wang et al. 2008; Xie et al. 2014; Xiong et al. 2014; Yao et al. 2014b), having the ability to dissociate NO and promote the de-NO_x efficiency. The concept of catalytic

domains, $-M_1^{x+}-\square-M_2^{y+}-$, was proposed (Yao et al. 2014b). Surface oxygen vacancies (SOV) and surface synergetic oxygen vacancies (SSOV) were found have a good catalytic activity for the NO-CO reaction. SSOV has better activity than SOV due to the influence of steric effect (Li et al. 2011a; Lv et al. 2013; Lv et al. 2012; Xiong et al. 2014; Yao et al. 2014a; Yao et al. 2014b). A large number of bimetallic catalysts were investigated. Cu-based catalysts have received extensive attention among transition bimetallic catalysts. The influence factors of catalytic activity, reaction mechanisms, and the effects of atmosphere conditions are summarized as follows.

One component of the bimetallic catalysts will have an effect on the other component, or both will produce a synergistic effect. CuO-CeO_2/MgO-Al_2O_3 catalyst showed a better catalytic performance, water resistance, and sulfur resistance than either CuO/MgO-Al_2O_3 catalyst or CeO_2/MgO-Al_2O_3 catalyst, due to the synergistic effect of Cu and Ce (Wen and He 2002). The Cu^+ and oxygen vacancies are beneficial to the adsorption of CO and NO, respectively, thereby promoting the catalytic activity. In the Cu-Ce/carbon nanotube (CNT) catalyst, the high electronegativity of Ce can promote the formation of Cu^+ (Gholami and Luo 2018). Among Cu/CeO_2, Cu/Fe_2O_3, and Cu/CeO_2-Fe_2O_3 catalysts, the existence of Fe promotes the adsorption of NO on Cu, accepts the O atom generated by the dissociation of NO, and inhibits the formation of −NCO species (Zhang et al. 2018c). However, excessive Fe changes the structure of the catalyst and inhibits the adsorption of CO. On the CuO-V_2O_5/γ-Al_2O_3 catalyst, the addition of V facilitates the dispersion of CuO, the adsorption of CO, and the dissociation of NO (Xiong et al. 2014). On the CuO-CoO_x/γ-Al_2O_3 catalyst, the synergistic interactions between the Cu and Co species resulted in more SSOVs (Cu^+-□-Co^{2+}) and a higher catalytic activity (Zhang et al. 2018a). On the CuO-CoO/γ-Al_2O_3 catalyst, both Cu and Co can provide adsorption sites for NO and the SSOV (Cu^+-□-Co^+) is the key to obtaining higher activity (Lv et al. 2013).

Pretreatment has a promoting effect on the NO-CO reaction for bimetallic catalysts. After the CO pretreatment on CuO/CeO_2 catalyst, the NO-CO reaction activity was improved (Gu et al. 2014), in that Cu^+/Cu^0 appeared on the catalyst surface, and the oxygen vacancy content was also improved. Cu^+ can adsorb CO, and oxygen vacancies can dissociate NO. CuO-CoO/γ-Al_2O_3 catalyst can generate SSOVs (Cu^+-□-Co^{2+}) after CO pretreatment, benefiting the NO-CO reaction (Lv et al. 2013). For CuO-V_2O_5/γ-Al_2O_3 catalysts, CO pretreatment can give better NO-CO reaction activity, because CO pretreatment can convert Cu^{2+} to Cu^+ at 300 °C and convert Cu^{2+} to Cu^0 at 500 °C (Xiong et al. 2014). CuO-MnO_x/TiO_2 catalyst has a better NO-CO reaction activity and N_2 selectivity than single-metal catalysts, and CO pretreatment can improve catalytic performance due to the generation of more oxygen vacancies and active centers (Sun et al. 2015). The mechanism of oxygen vacancy generation is given in Eqs. 33–35 (Sun et al. 2015). The results are consistent with other studies (Gholami and Luo 2018; Gu et al. 2014; Li et al. 2011a; Lv et al. 2013; Qin et al. 2016; Xiong et al. 2014).

$$Cu^{2+}-\square-Cu^{2+}\xrightarrow{CO,\ \text{low temperature}}Cu^{+}-\square-Cu^{+} \quad (33)$$

$$Cu^{2+}-\square-Mn^{4+}\xrightarrow{CO,\ \text{low temperature}}Cu^{+}-\square-Mn^{3+} \quad (34)$$

$$\xrightarrow{CO,\text{high temperature}}Cu^{+}-\square-Mn^{2+}$$

$$Cu^{2+}-\square-Mn^{3+}\xrightarrow{CO,\ \text{low temperature}}Cu^{+}-\square-Mn^{3+} \quad (35)$$

$$\xrightarrow{CO,\text{high temperature}}Cu^{+}-\square-Mn^{2+}$$

Three kinds of reaction mechanisms on the bimetallic catalysts for the NO-CO reaction have been proposed. Firstly, the adsorption and dissociation of NO occur on the metal sites on the bimetallic catalysts. The NO-CO reaction occurs only in the presence of $NO_{(ads)}$ and $CO_{(ads)}$. This is consistent with previous studies that show that the dissociation of NO has a high energy barrier, and the adsorption of CO by a vacant adjacent site is necessary to initiate the reaction (Campbell and White 1978; Iliopoulou et al. 2005b; Oh 1986; Rainer et al. 1997). On the CuO-CoO/γ-Al_2O_3 catalyst, NO adsorbs preferentially on the Co site and CO adsorbs preferentially on the Cu site (Lv et al. 2013). On the Cu/CeO_2, Cu/Fe_2O_3, and Cu/CeO_2-Fe_2O_3 catalysts, the reaction mechanism for the NO-CO reaction was as follows (Zhang et al. 2018c). On Cu/CeO_2 catalyst, NO adsorbs on the Cu site and CO adsorbs on the Ce site. On Cu/CeO_2-Fe_2O_3 catalyst, NO adsorbs on the Fe^{3+} and Cu^{2+} sites, and CO adsorbs on the Ce^{3+} and Cu^+ sites. On both catalysts the reaction intermediates are −NCO species at low temperatures and are N_2O at high temperatures. On the Cu/Fe_2O_3 catalyst, NO adsorbs on the Fe site and CO adsorbs on the Cu site. The reaction intermediates are N_2O. The generation of −NCO species is inhibited, due to the large specific gravity of Fe.

Secondly, the adsorption and dissociation of NO can also occur on oxygen vacancies on the bimetallic catalysts. On the CuO/CeO_2 catalyst, NO_x adsorbed on the oxygen vacancies is more susceptible to dissociation than NO_x adsorbed on Cu, CO is more easily adsorbed on the Cu site than NO, and the main product is NO_2^- (Martínez-Arias et al. 2012). At low temperatures, NO can be converted to nitrosyls (−NO) on CuO, whereas it will react to form chelating NO_2^- and hyponitrite species on the CeO_2. On the Cu-Ce/CNT catalyst, the interaction between surface oxygen vacancies and Cu^+ species enhanced the activity of the catalyst (Gholami and Luo 2018). The reaction mechanism was proposed that CO adsorbed on Cu^+ and that NO dissociated on oxygen vacancies, as shown in Fig. 4. The reaction mechanism of CuO-V_2O_5/γ-Al_2O_3 catalyst with SSOVs as catalytic active centers is shown in Fig. 5. Compared with V^{4+}, CO is more easily adsorbed on Cu^+, combining with free radicals [O] reduced by the NO decomposed on adjacent oxygen vacancies to generate CO_2. The free radical [N] reacts with NO or CO to

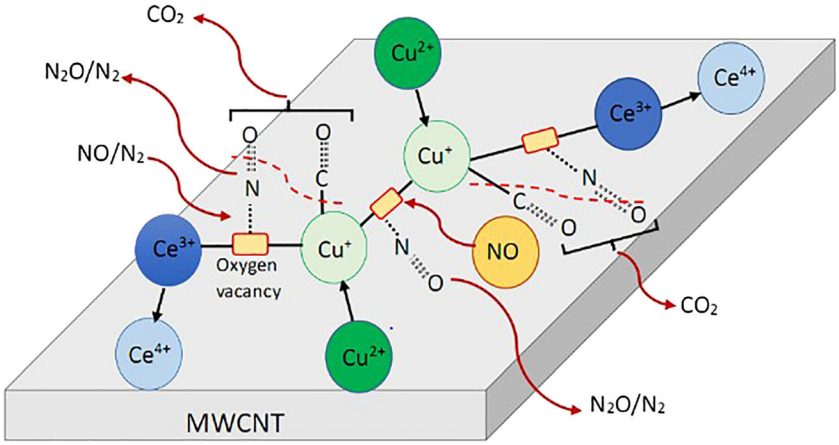

Fig. 4 The mechanism of the NO-CO reaction on Cu-Ce/CNT catalyst (Gholami and Luo 2018). Copyright 2018, American Chemical Society

generate N_2O or –NCO species, respectively. Otherwise, the [N] themselves combine to generate N_2.

Finally, the adsorption and dissociation of NO can occur on both oxygen vacancies and metal sites on the bimetallic catalysts. The mechanism of the NO-CO reaction on CuO-CoO_x/γ-Al_2O_3 catalyst was proposed as shown in Fig. 6 (Zhang et al. 2018a). At 25-150 °C, NO will preferentially adsorb on the catalyst due to its unpaired electrons to generate several kinds of NO_3^- species, which further inhibit the adsorption of CO. At 175 °C, the CO in the atmosphere will reduce the catalyst to generate Cu^+ and oxygen vacancies, which can be used for CO adsorption and dissociation of NO, respectively, with intermediate species of N_2O and −NCO. At 200–325 °C, more Cu^+ and oxygen vacancies are generated. Since the oxygen vacancy can weaken the N-O bond to promote the dissociation of NO, no adsorbed NO_x can be observed on the catalyst surface. In addition, oxygen vacancy promotes the further reaction of N_2O and −NCO to form N_2 to improve the N_2 selectivity.

The atmospheric conditions seriously affect the NO-CO reaction performance on the bimetallic catalysts. Cu-Cr/AC catalyst prepared by the coprecipitation method has both NO-CO reaction activity and CO catalytic oxidation activity, so the NO reduction by CO was suppressed in the presence of O_2 (Stegenga et al. 1993). The activity of the NO-CO reaction on Cu-Ce/CNT catalyst was greatly decreased by O_2 (Gholami and Luo 2018). At a high O_2 concentration of O_2/CO>0.6, the Cu-Ce/CNT catalyst can

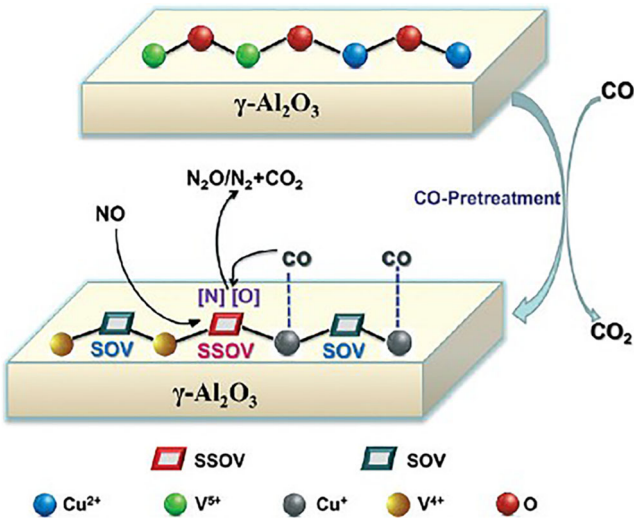

Fig. 5 The mechanism of the NO-CO reaction on CuO-V_2O_5/γ-Al_2O_3 catalyst (Xiong et al. 2014). Copyright 2014, Royal Society of Chemistry

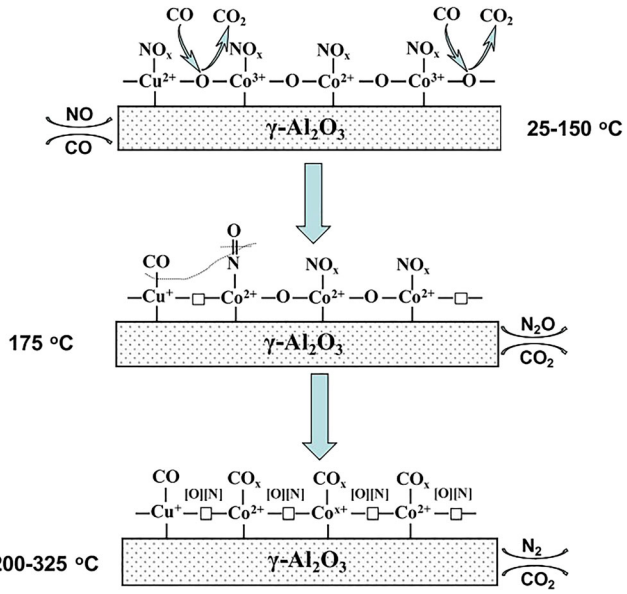

Fig. 6 The mechanism of the NO-CO reaction on CuO-CoO_x/γ-Al_2O_3 catalyst (Zhang et al. 2018a). Copyright 2018, Elsevier

effectively catalyze CO oxidation. Therefore, the NO-CO reaction does not occur. O_2 is more easily reduced than NO on CuO/CeO_2 catalyst and preferentially reacts with CO, thereby inhibiting the process of NO reduction by CO (Zhang et al. 2017b).

Non-Cu-based bimetallic catalysts

In addition to Cu-based bimetallic catalysts, other bimetallic catalysts have also been extensively studied. Fe-Co/activated semi-coke (ASC) bimetallic catalysts for the NO-CO reaction have been deeply studied (Cheng et al. 2018; Cheng et al. 2016a; Cheng et al. 2016b; Wang et al. 2017a; Wang et al. 2017b; Wang et al. 2017c), with the catalytic mechanism proposed. The SSOVs are formed in the Fe-Co/ASC catalyst, and the metal with higher electronegativity acts as a redox site, while metals with lower electronegativities serve to assist in the reaction, as shown in Fig. 7. Fe captures an electron from the CO and transmits it to NO adsorbed on Co through a coordinated oxygen vacancy, thereby weakening the N-O bond and promoting the dissociation of the NO. CO adsorbed on the catalyst forms a bidentate CO_3^{2-}, and NO adsorbed on the catalyst surface forms the important intermediate NO_2^-. Below 200 °C, the intermediate NO_2^- further evolves to NO-NO_3^-, which reacts to generate N_2O. Above 200 °C, the intermediate NO_2^- is converted to bidentate NO_3^-, which further evolves to produce N_2 and chelating NO_3^-. H_2O and SO_2 can inhibit the NO-CO reaction on Fe-Co/ASC catalyst. H_2O can occupy the NO adsorption sites and CO adsorption sites, thereby inhibiting the formation of carbonates and nitrates. SO_2 can deactivate the catalyst by forming sulfite with metal ions. When both SO_2 and H_2O are present, a sulfate species is formed which deposits on the surface of the catalyst, causing an irreversible deactivation of the catalyst.

The NO-CO reaction mechanism on the Fe_2O_3-CeO_2-$Ti_{0.5}Sn_{0.5}O_2$ catalyst is shown in Fig. 8. Fe^{2+} produced by reduction of Fe^{3+} is the main active site. NO adsorbs on the surface of the catalyst to form several types of NO_2^- species. As the temperature increases, the bridging bidentate NO_3^- species transform into chelating nitro species, which reacts with gaseous CO to produce CO_2 and N_2O. When the temperature is above 200 °C, the NO adsorbed on Fe^{2+} will react with the carbonate species adsorbed on the surface of the catalyst to produce CO_2 and N_2.

On a $Ce_xSn_{1-x}O_2$ catalyst, the addition of Sn^{4+} to the CeO_2 lattice will reduce the crystal size, increase the lattice strain, and improve the reducibility, thereby improving the catalyst performance (Yao et al. 2014b). The NO-CO reaction mechanism was proposed that NO adsorbs on oxygen vacancies which catalyze NO dissociation to generate free [N] and [O] radicals. [O] will combine with CO adsorbed on Ce^{3+} to generate CO_2, while the [N] combines with each other to generate N_2 or combines with NO to generate N_2O. The Ce^{3+} site is considered an activation and adsorption site of CO, which can adsorb CO_x species (Boaro et al. 2004; Hailstone et al. 2009; Li et al. 2011a; Luo et al. 2007; Song et al. 2007; Wu et al. 2004; Yin et al. 2002; Zhang et al. 2018c).

$Ce_{0.67}Sn_{0.33}O_2$ catalyst has a higher NO-CO reaction activity than CeO_2. This is attributed to the small particle size, the large specific surface area, and the high content of surface Ce^{3+} and oxygen vacancies (Yao et al. 2013b). These factors promote the contact of the reaction molecule with the catalyst. The mechanism of the NO-CO reaction was proposed. At 25 °C, NO preferentially adsorbs on the surface of the catalyst to generate NO_2^- and NO_3^- species. At 200 °C, a small amount of NO will desorb, transform, and decompose, releasing a small number of sites for CO adsorption. At this time, a small amount of N_2O, N_2, and CO_2 will be produced, but the de-NO_x efficiency and the N_2 selectivity are both low. Above 250 °C, the catalyst surface will generate a large number of Ce^{3+} and oxygen vacancies due to the reduction of CO in the atmosphere. Ce^{3+} provides a site for the adsorption of CO, and oxygen vacancies promote the dissociation of NO. Thus, a large amount of N_2 and CO_2 are produced, and the de-NO_x efficiency is improved.

The CeO_2-MnO_x/Al_2O_3 catalyst has higher activity than the CeO_2-MnO_x catalyst (Yao et al. 2016). The addition of Al_2O_3 as a carrier reduces the grain size, increases the specific surface area and pore volume, and then further increases the contact between the catalyst and the reaction molecules. Furthermore, the numbers of Ce^{3+} and Mn^{4+} are also increased, which benefits the adsorption of CO and the desorption, conversion, or dissociation of NO, respectively. The NO-CO reaction mechanism is shown in Fig. 9. NO preferentially adsorbs on the Mn site to form NO_2^- and NO_3^- due to the unpaired electrons at the Mn^{n+} site at low temperatures below 350 °C. Meanwhile, the adsorption of CO is suppressed. The gaseous CO reacts with the adsorbed NO species to form a large amount of N_2O and a small amount of N_2. However, gaseous CO can react with catalyst at high temperatures above 350 °C. This results in the reduction of the catalyst to form more Ce^{3+} and oxygen vacancies, thus promoting the adsorption of CO and the dissociation of NO, respectively. Therefore, NO can be

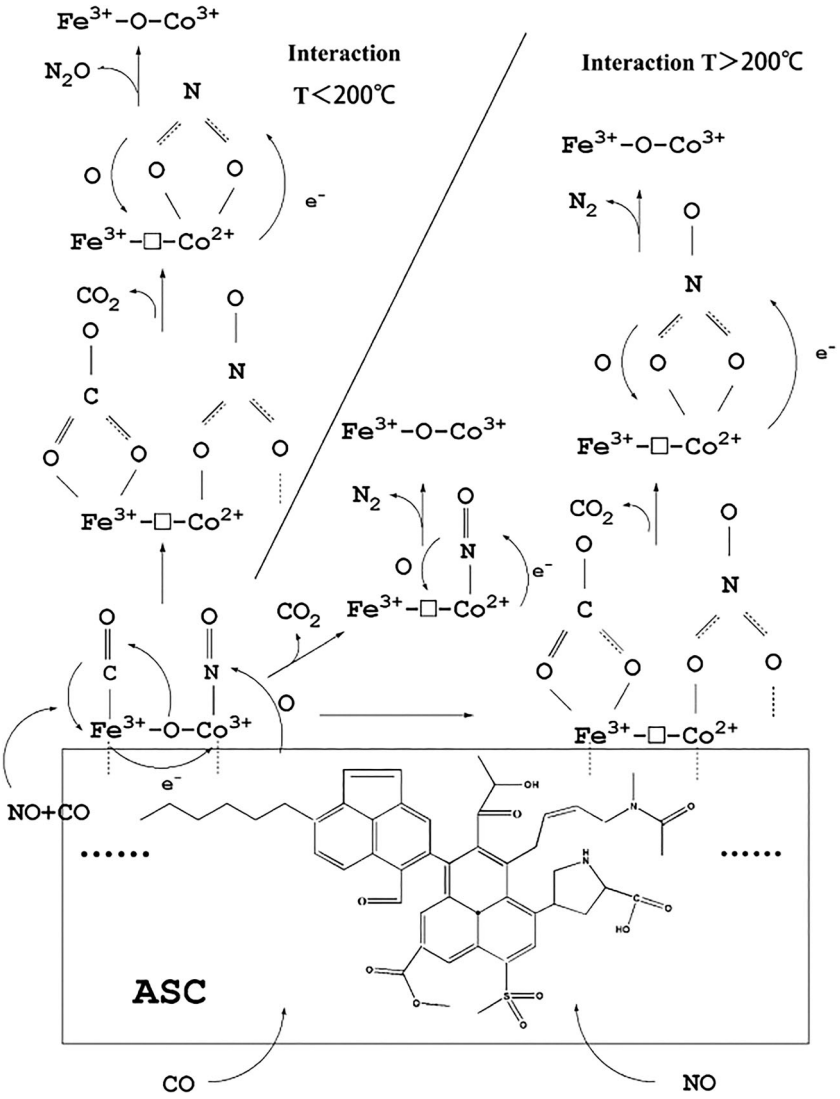

Fig. 7 The mechanism of the NO-CO reaction on Fe-Co/ASC catalyst (Wang et al. 2017a). Copyright 2017, Elsevier

dissociated into [N] and [O] to react with adsorbed CO forming a large amount of N_2 and CO_2, along with a small amount of N_2O. The N_2O will be further converted to N_2 at high temperature.

Summary

Based on the previous studies, it was found that the CO adsorption activation centers include Fe^{2+}, Fe^{3+}, Cu^{+}, Cu^{2+}, Ce^{3+}, and Ce^{4+}, while the NO adsorption activation centers include Fe^{2+}, Fe^{3+}, Cu^{+}, Cu^{2+}, Co^{2+}, Co^{3+}, Mn^{4+}, V^{4+}, Mo^{4+}, and oxygen vacancies. The NO-CO reaction follows the L-H mechanism accompanied by electron transfer. The rate-determining step of the NO-CO reaction is the dissociation of NO which has a high energy barrier. The catalytic activity of the catalyst for the NO-CO reaction depends on the surface oxygen vacancies, the dispersion of metal oxides, and the redox of the catalyst.

Performances of the partial typical transition metal catalysts for the NO-CO reaction are summarized in Table 3. Through extensive research on transition metal catalysts, the mechanism of the NO-CO reaction using SOV and SSOV as active centers has been generally accepted by researchers. The mechanism of the NO-CO reaction on transition metal catalysts can be summarized into three types. For the first case, the oxygen vacancy adsorbs and dissociates NO, and the adjacent metal site adsorbs CO, which is shown in Fig. 10a. The second type is that in which one metal site connected with oxygen vacancies adsorbs NO and another metal site connected with oxygen vacancies adsorbs CO. Electrons in CO can be transferred to the antibonding orbital of NO through oxygen vacancies. As a result, the dissociation of NO was improved, as shown in Fig. 10b. The last

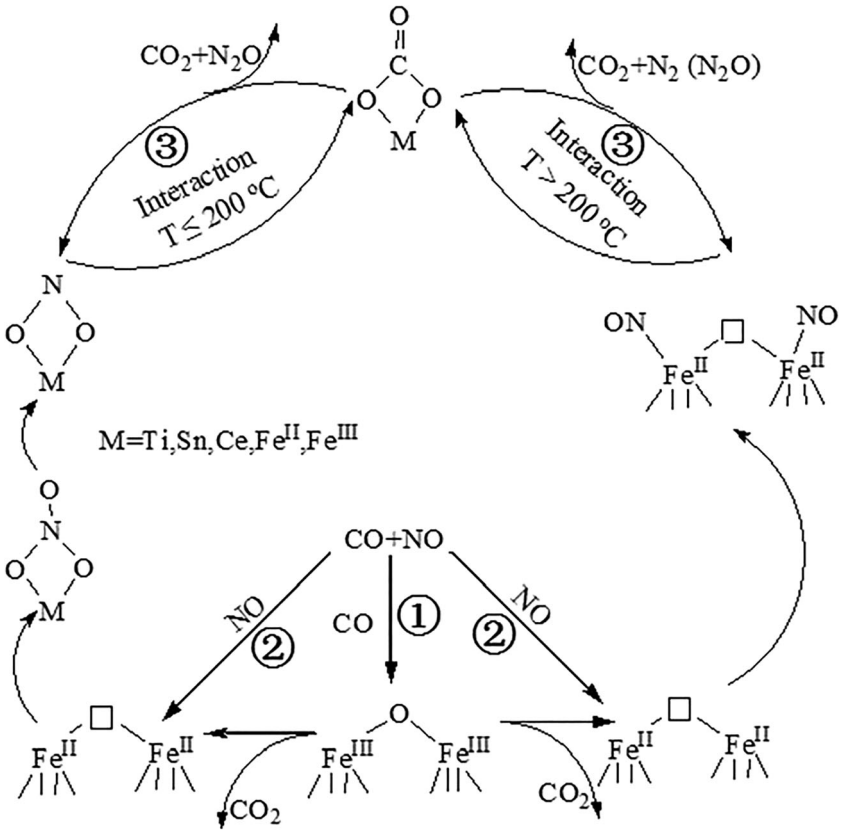

Fig. 8 The mechanism of the NO-CO reaction on Fe_2O_3-CeO_2-$Ti_{0.5}Sn_{0.5}O_2$ catalyst (Dong et al. 2014). Copyright 2014, Royal Society of Chemistry

one is that in which two adjacent metal active sites on the catalyst surface adsorb NO and CO respectively, similar to noble metal catalysts, as shown in Fig. 10c. This mechanism is mostly proposed in the transition mono-metallic catalysts. In any of the three reaction mechanisms mentioned above, oxygen vacancies can participate directly or indirectly in the catalytic reaction. In addition, due to the steric effect, the SSOV has higher catalytic activity than SOV, which is also the reason why the transition bimetallic catalysts have a better performance than mono-metallic catalysts.

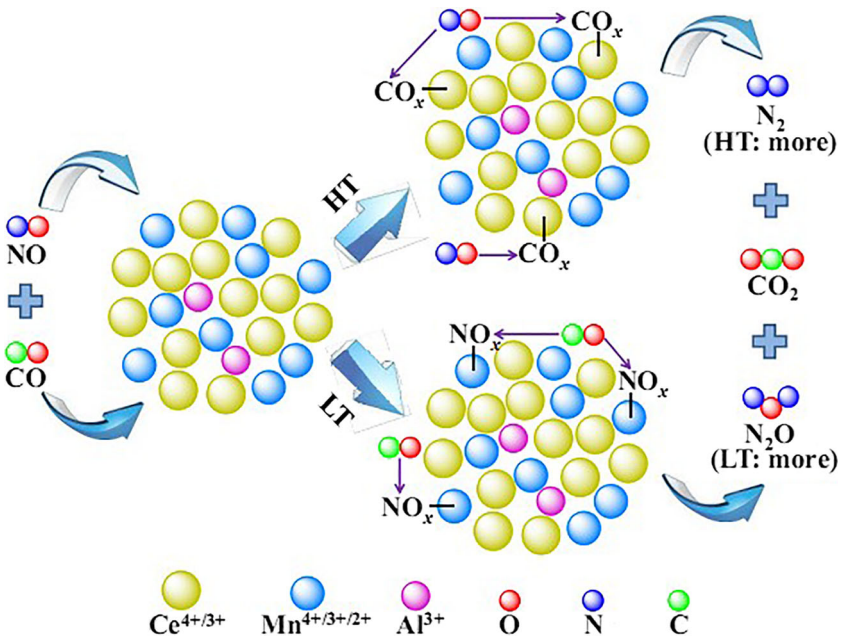

Fig. 9 The mechanism of the NO-CO reaction on CeO_2-MnO_x-Al_2O_3 catalyst (Yao et al. 2016). Copyright 2016, Elsevier

Table 3 Activity of various transition metal catalysts for the NO-CO reaction

Catalyst	Reaction conditions					T_{20}[f] (°C)	T_{50}[g] (°C)	T_{max}[h] (°C)	NO conversion (%)	N_2 selection (%)	References
	Temperature range(°C)	GHSV[d] or WHSV[e]	NO (ppm)	CO (ppm)	O_2 (%)						
Fe-Co/N-ASC	150–300	12,000 h^{-1}	800	1600	\		200	300	99.1		(Sun et al. 2019)
Cu/$SmCeO_2/TiO_2$[a]	150–350	10,000 h^{-1}	500	10,000	10	\		225	100	\	(Venegas et al. 2019)
MnO_x/TiO_2	200	50,000 h^{-1}	400	400	2	\	\	200	95	\	(Boningari et al. 2018)
Cu/Fe_2O_3–CeO_2/ZrO_2	75–250	30,000 h^{-1}	800	1600	\	85	105	175	99	49	(Zhang et al. 2018b)
Cu-Ce/CNT	140–260	12,600 h^{-1}	250	5000	\	150	170	240	90		(Gholami and Luo 2018)
Fe-Co/ASC-KOH	150–350	20,000 h^{-1}	800	2000	\		150	250	95	75	(Cheng et al. 2018)
CuO/CeO_2-Fe_2O_3	50–200	30,000 h^{-1}	800	1600	\	85	110	175	95	35	(Zhang et al. 2018c)
CuO-CoO_x/γ-Al_2O_3	150–350	12,000 ml g^{-1} h^{-1}	50,000	100,000	\	160	200	300	97	100	(Zhang et al. 2018a)
Fe/ZSM-5	250–400	5000 h^{-1}	1000	2000	\	\		350	100	100	(Cheng et al. 2017)
NiO-CeO_2	100–300	9000 ml g^{-1} h^{-1}	25,000	50,000	\	110	135	175	100	2	(Tang et al. 2017)
Fe-Co/ASC	150–350	20,000 h^{-1}	1000	5000	1	250	\	300	35	25	(Cheng et al. 2016a)
Fe-Co/ASC	100–350	6000 h^{-1}	1000	2000	\	125	150	200	95	100	(Wang et al. 2017a)
Fe-Co/ASC	150–350	6000 h^{-1}	1000	2000	\	\	170	300	95	100	(Wang et al. 2017b)
Fe-La/ASC	150–350	6000 h^{-1}	1000	2000	\	250	275	350	90	100	(Wang et al. 2017b)
Fe-Ce/ASC	150–350	6000 h^{-1}	1000	2000	\	220	260	325	85	100	(Wang et al. 2017b)
CeO_2-MnO_x-Al_2O_3	100–450	12,000 ml g^{-1} h^{-1}	50,000	100,000	\	240	280	400	100	98	(Yao et al. 2016)
$CuO/Ce_{20}Zr_1O_x$	100–350	24,000 ml g^{-1} h^{-1}	50,000	100,000	\	105	118	200	96	68	(Deng et al. 2016)
$Ce_{0.8}Fe_{0.2}O_2$	100–350	60,000 ml g^{-1} h^{-1}	5000	5000	\	155	190	350	96	100	(Brackmann et al. 2016)
$La_{0.8}Ce_{0.2}Mn_{0.3}Fe_{0.7}O_3$	100–450	12,000 h^{-1}	3000	3000	\	200	250	400	98	93	(Tarjomannejad et al. 2016)
Cu-Mn/TiO_2	200–350	12,000 h^{-1}	50,000	100,000	\	250	280	350	95	95	(Sun et al. 2015)
Cu/$AlPO_4$	200–500	120,000 ml g^{-1} h^{-1}	2000	15,000	0.65	260	280	320	95	\	(Kacimi et al. 2015)
CuO-MnO_x/TiO_2	200–350	12,000 h^{-1}	50,000	100,000	\	260	280	350	98	95	(Sun et al. 2015)
Cu/TiO_2-CeO_2	150–400	24,000 ml g^{-1} h^{-1}	50,000	100,000	\	\	220	350	100	100	(Deng et al. 2015)
$Ce_xSn_{1-x}O_2$	150–400	12,000 ml g^{-1} h^{-1}	50,000	100,000	\	250	350	400	75	100	(Yao et al. 2014b)
CuO/CeO_2	100–200	12,000 h^{-1}	50,000	100,000	\	\	\	200	90	75	(Gu et al. 2014)
CuO-V_2O_5/γ-Al_2O_3	150–400	24,000 ml g^{-1} h^{-1}	50,000	100,000	\	225	275	350	98	95	(Xiong et al. 2014)
$CuO/CeO_2/\gamma$-Al_2O_3	150–400	12,000 h^{-1}	50,000	100,000	\	175	275	350	100	100	(Ge et al. 2014)
Fe_2O_3-CeO_2-$Ti_{0.5}Sn_{0.5}O_2$	150–400	24,000 ml g^{-1} h^{-1}	50,000	100,000	\	210	265	400	97	100	(Dong et al. 2014)
Fe/TiO_2	250–500	75,000 h^{-1}	5000	5000	\	345	470	500	59	\	(Sierra-Pereira and Urquieta-Gonzalez 2014)
Cu/MCM-41	227–450	48,000 ml g^{-1} h^{-1}	250	750		332	392	450	75	\	(Patel et al. 2014)
CuO-CoO/γ-Al_2O_3	150–250	24,000 h^{-1}	25,000	50,000	\	\		250	95	90	(Lv et al. 2013)
CuO/Al_2O_3	100–400	12,000 h^{-1}	50,000	100,000	\	130	180	250	100	90	(Yao et al. 2013a)
CuO/CeO_2	100–325	24,000 ml g^{-1} h^{-1}	50,000	100,000	\	120	185	300	95	100	(Yao et al. 2013c)
$Ce_{0.67}Sn_{0.33}O_2$	100–400	12,000 ml g^{-1} h^{-1}	50,000	100,000	\	200	280	400	82	100	(Yao et al. 2013b)
CuO-CoO/γ-Al_2O_3	100–325	12,000 h^{-1}	25,000	50,000	\	100	150	300	95	95	(Lv et al. 2012)
CuO/ZrO_2	100–450	12,000 h^{-1}	50,000	100,000	\	175	250	450	100	100	(Yu et al. 2012)
Cr/C[b]	350–600	0.98 g s μmol^{-1}	200	10,000	3	450	520	600	85	\	(Rosas et al. 2010)
CuO/CeO_2	100–400	120,000 ml g^{-1} h^{-1}	50,000	100,000	\	100	150	400	57	100	(Liu et al. 2010)
Cu/CeO_2	150–400	32,000 h^{-1}	5000	5000	\	\	\	300	95	\	(Chen et al. 2010a)
Cu/CeO_2	150–400	32,000 h^{-1}	5000	5000	\	\		300	96	\	(Chen et al. 2010a)
Cu/MgO-CeO_2	150–400	16,000 h^{-1}	5000	6000	\	\	\	250	100	100	(Chen et al. 2009a)
Mn/TiO_2	200	50,000 h^{-1}	400	400	2		\	200	95		(Sreekanth and Smirniotis 2007)
Ag-Co/CeO_2	100–600	12,000 h^{-1}	2500	12,500	0.5	140	180	300	100	95	(Zhang et al. 2007a)
$La_{0.8}Ce_{0.2}Cu_{0.4}Mn_{0.6}O_3$	150–500	20,000 h^{-1}	10,000	10,000	\	180	220	300	100	95	(He et al. 2007)
6%CuO-10%ZrO_2/TiO_2	100–450	5000 h^{-1}	60,000	60,000	\	100	210	350	100	100	(Jiang et al. 2004)
CoS_{2-x}/TiO_2	250–450	8000 h^{-1}	1025	2085	\	\	\	400	97.5	\	(Zhang and Yang 2003)
15%$CuO/Ce_{0.8}Zr_{0.2}O_2$	100–500	0.1125 g s cm^{-3}	60,000	65,000	\	180	235	350	100	100	(Ma et al. 2003)
0.5%Cu/Al_2O_3	300–500	30,000 h^{-1}	10,000	10,000	0.5	\	\	500	15.4	100	(Yamamoto et al. 2002)
Co-Cr/AC[c]	127–377	45,000 h^{-1}	2000	2000	\	252	287	377	100	\	(Stegenga et al. 1993)

[a] The activity was evaluated in the presence of 500 ppm naphthalene

[b] The activity was evaluated in the presence of 2000 ppm SO_2 and 2000 ppm C_3H_6

[c] The activity was evaluated in the presence of 3% H_2O

[d] GHSV means gaseous hourly space velocity (h^{-1})

[e] WHSV means weight hourly space velocity (ml g^{-1} h^{-1})

[f] T_{20} represents the temperature when the efficiency is 20%

[g] T_{50} represents the temperature when the efficiency is 50%

[h] T_{max} represents the temperature when the efficiency is maximum

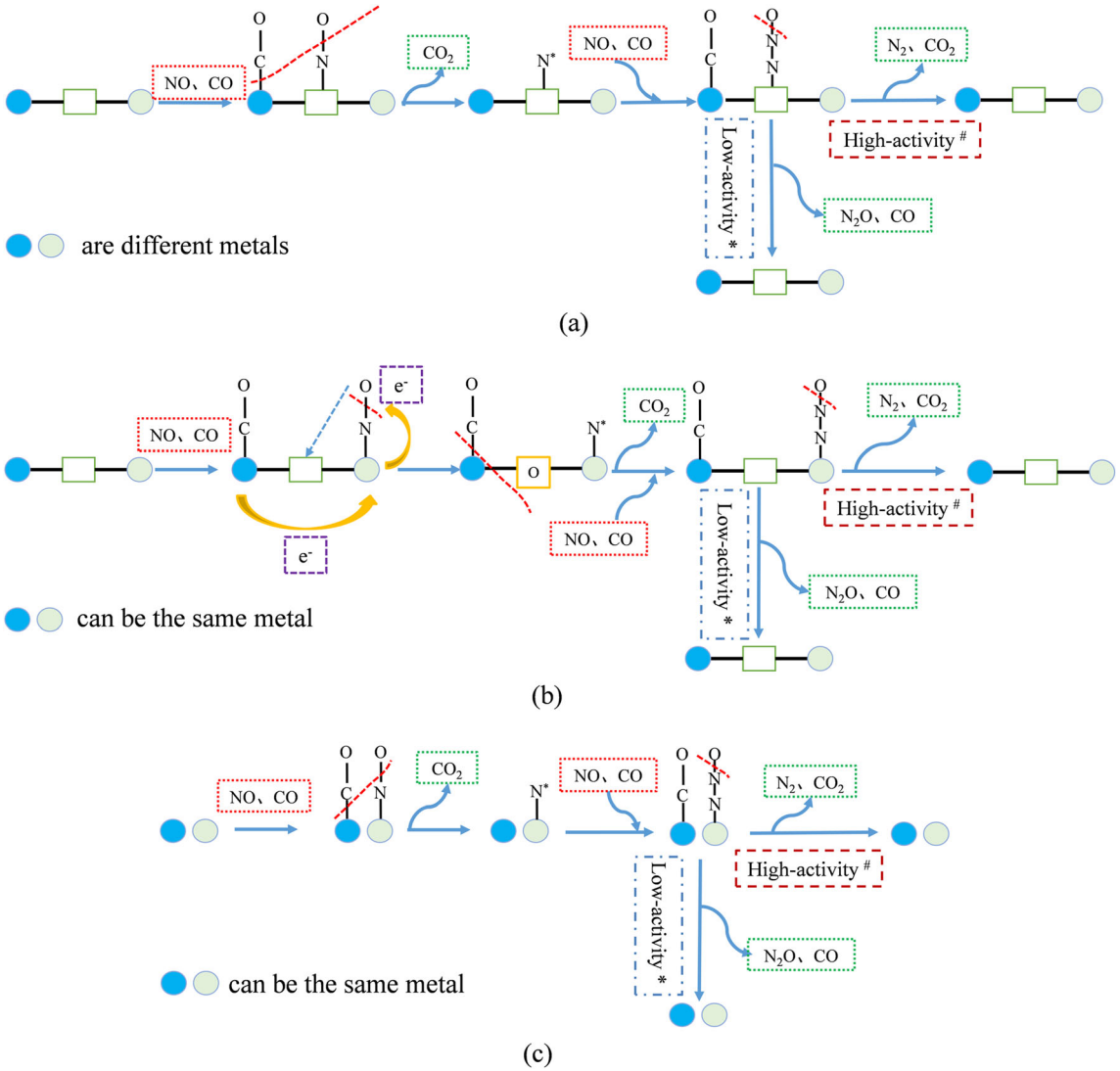

Fig. 10 NO-CO reaction mechanism for transition bimetallic catalysts

The effect of atmosphere is a bottle neck for transition metal catalysts to apply in NO-CO reaction. Experimental study on the effects of H_2O and SO_2 on NO-CO reaction activity has not been carried out. O_2 has a serious negative effect on NO-CO reaction, especially on surface oxygen vacancies. Among the transition metal catalysts, the Cu-based catalysts have the highest NO-CO reaction activity in the absence of O_2. In addition, the low-temperature activity and N_2 selectivity of the catalyst should be considered to obtain a catalyst suitable for industrial flue gas. The application of transition metal catalysts to industrial flue gas is difficult in light of current research progress.

*N-O bond dissociation rate in $N_2O_{(ads)}$ is lower than $N_2O_{(ads)}$ desorption rate

#N-O bond dissociation rate in $N_2O_{(ads)}$ is higher than $N_2O_{(ads)}$ desorption rate

Challenges and potential

Although noble metal catalysts and transition metal catalysts have been extensively researched for the NO-CO reaction, there are still some problems in the application to industrial flue gas of the reduction of NO by CO. The challenges and the solutions currently are summarized as follows.

Effect of O_2

CO-SCR was initially applied to motor vehicle exhaust, and in recent years, it has gradually been applied to industrial flue gas. The characteristics of gas from motor vehicles and industry are compared in Table 4. The O_2 content in the industrial flue gas is much higher than that in the motor vehicle exhaust. Different from motor vehicle exhaust, the O_2 content is also more than the CO content in industrial flue gas. Even when the O_2 content

Table 4 Characteristics of various industrial flue gases

Components	Motor vehicle exhaust	Sintering flue gas	Pelletizing flue gas	Coke oven flue gas
O_2 (%)	0.1–2	12–18	14–18	4–8
CO (%)	1–8	0.6–1.2	0.6–1.2	0.04–0.2
H_2O (%)	5–10	8–12	8–12	5–17.5
NO_x (mg/m^3)	500–4000	200–350	200–300	300–800
SO_2 (mg/m^3)	< 15	300–2000	400–1000	50–200
Temperature (°C)	200–600	120–180	110–180	180–230

is higher than that of CO, Ir-based catalysts can also achieve the reduction of NO by CO in the presence of SO_2 and H_2O. However, the high concentrations of O_2 will strongly inhibit the NO-CO reaction, so that CO will preferentially react with O_2, and the N_2 selectivity is partially lost. The inhibition by O_2 include ① inhibiting the dissociation of NO (Cheng et al. 2016a; Fink et al. 1991; Makeev and Nieuwenhuys 1998; Makeev and Peskov 2013; Oh et al. 1986; Patel et al. 2014; Reddy and Khanna 2004; Shi et al. 2002; Wang et al. 2003) due to the increase in the oxygen concentration on the catalyst surface, which can damage or occupy the active center, such as oxidized metal sites or oxygen vacancies (Cheng et al. 2018; Cheng et al. 2016a; Gholami and Luo 2018; Hamada and Haneda 2012; Makeev and Peskov 2013; Patel et al. 2014; Reddy and Khanna 2004; Zhang et al. 2017a) and ② consuming CO through the oxidation of CO to CO_2 (Cheng et al. 2016a; Gholami and Luo 2018; Hamada and Haneda 2012; Li et al. 2012; Li et al. 2011b; Li et al. 2014b; Ming et al. 1997; Sreekanth and Smirniotis 2007; Stegenga et al. 1993; Wang et al. 2017a; Wang et al. 2017c; Zhang et al. 2017b). Therefore, the application of the reduction of NO by CO in industrial flue gas is difficult. At present, the solutions given by researchers are as follows.

- Use a new type of reactor as shown in Fig. 11. The rotary reactor first adsorbs NO from the flue gas to the catalyst and then performs the NO-CO reaction in an oxygen-free atmosphere (Cheng et al. 2016b). This method is similar to the principle of NO_x storage reduction (NSR). However, additional CO and a new reactor are needed.
- Design catalyst with good oxygen resistance. It has been found that Ir preferentially adsorbs NO in the presence of O_2, thereby realizing the reduction of NO by CO. Recently, some researchers have proposed that MnO_x/TiO_2 and Cu/$SmCeO_2$/TiO_2 (Venegas et al. 2019) catalysts have realized the reduction of NO by CO in the presence of O_2. However, the feasibility and the great selectivity of NO reduction by CO require to be further studied.
- Deposit the reducing agent such as urea or naphthalene on the surface of the catalyst (Liu et al. 2017; Venegas et al. 2019). CO oxidation, NO-CO reaction, and urea-SCR or reduction of NO by naphthalene will then be carried out simultaneously, as shown in Fig. 12. Urea-SCR can reduce the content of NO_x in the presence of O_2. However, this method requires a reductant introduced on the catalyst.

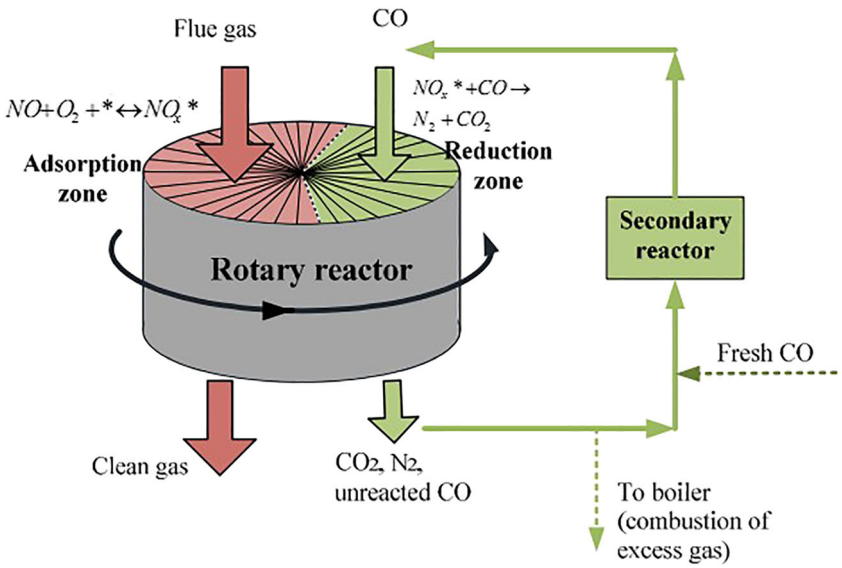

Fig. 11 A new type of reactor for NO reduction by CO (Cheng et al. 2016b). Copyright 2016, Royal Society of Chemistry

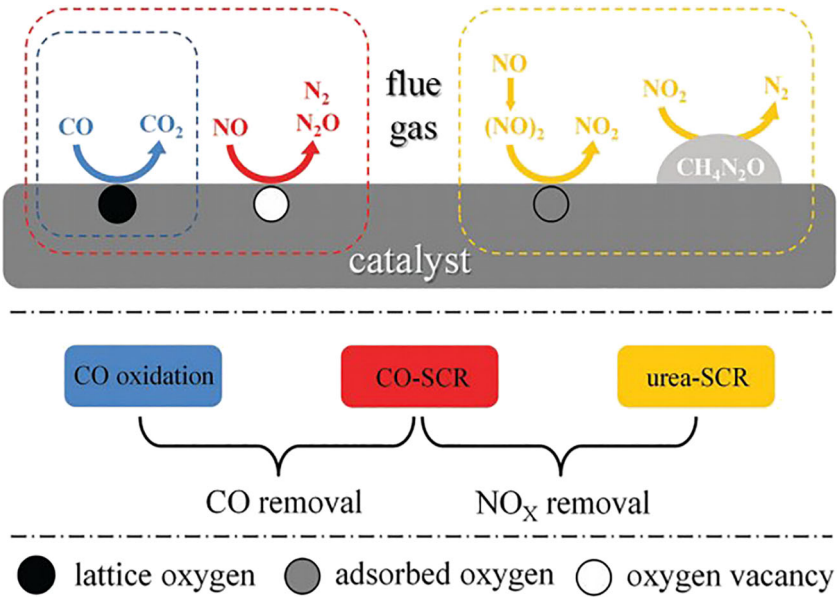

Fig. 12 Simultaneous removal mechanism of CO and NO_x on the catalyst with a deposited reducing agent (Liu et al. 2017). Copyright 2017, Royal Society of Chemistry

The methods mentioned above partially solve the inhibition of O_2 in industrial application, but the more economical and convenient solutions need to be developed.

Effect of temperature

There is a large difference in the temperatures of industrial flue gas and motor vehicle exhaust. The reduction of NO by CO in industrial flue gas is faced with the challenge of low temperature. When the temperature is below 200 °C, the noble metal catalysts cannot be used due to their weak activity and poor N_2 selectivity and the transition metal catalysts are difficult to apply due to their low N_2 selectivity. The idealized NO-CO reaction process is to produce N_2 and CO_2. The transformation of NO results in the intermediate products of −NCO species (Campbell and White 1978; Iliopoulou et al. 2005b; Lv et al. 2013; Martínez-Arias et al. 2012; Oh 1986; Rainer et al. 1997; Sun et al. 2009; Xiao et al. 2014; Xiong et al. 2014; Yang et al. 2011; Zhang et al. 2018c) or N_2O (Burch et al. 1994; Cheng et al. 2016a; Cho et al. 1989; Fink et al. 1991; Gu et al. 2014; Ilieva et al. 2015; Kotsifa et al. 2008; Lv et al. 2013; Mehandjiev and Bekyarova 1994; Oh 1986; Pirug 1977; Pirugand and Bonzel 1977; Shangguan et al. 1996; Shimokawabe and Umeda 2004; Sugi et al. 1975; Wang et al. 2003; Weisweiler et al. 2002; Xiong et al. 2014; Yang et al. 2011; Yao et al. 2014b; Zhang et al. 2018c), while not completely converted to N_2. Specifically, when the temperature is below 200 °C, more N_2O is produced and the N_2 selectivity of the catalyst is low.

In industrial applications, high N_2 selectivity and NO conversion can be obtained by increasing the flue gas temperature through heat exchangers, flue gas circulation sintering (FGCS) (Li et al. 2014a; Zhang et al. 2014), or flue gas recirculation (FGR) (Yu et al. 2017). The conversion of NO increases after the temperature of flue gas has been increased and the O_2 content of flue gas has been reduced. However, these methods require additional equipment, which will aggravate the cost problem. Therefore, catalysts with high activity and N_2 selectivity at low temperature need to be developed.

Conclusion

In this work, noble metal catalysts and transition metal catalysts used to catalyze the reduction of NO by CO are reviewed. Among Pd-, Pt-, Rh-, Ru-, and Ir-based noble metal catalysts, Ir shows excellent properties. The reduced state of Ir is an important prerequisite to ensure the high activity in the NO-CO reaction. For Ir-based catalysts, their own excellent antioxidant abilities and excellent water and sulfur resistance provide the possibility of application to industrial flue gas; however, the narrow catalytic reaction temperature window limits their extensive application.

Compared with noble metal catalysts, transition metal catalysts have attracted much attention. Cu-based mono-metallic catalysts show excellent performance. Cu can be used as both the CO adsorption site and NO adsorption dissociation site. The existence of oxygen vacancies can catalyze the dissociation of NO, which further improves the catalytic activity and the conversion of NO. In addition to mono-metallic catalysts, bimetallic catalysts have received extensive attention in recent years. Three different reaction mechanisms on bimetallic catalysts have been proposed. The adsorption and dissociation of NO can occur on the metal sites, the oxygen vacancies, or the both of them. Oxygen vacancies play an important role in the

NO-CO reaction. The activity of bimetallic catalysts is generally higher than that of mono-metallic catalysts due to the existence of surface synergetic oxygen vacancies. Cu-based catalysts have higher catalytic activity than the other transition metal catalysts. However, the oxygen vacancies and low-valence metal active sites in the transition metal catalysts are easily inhibited by O_2, which is a large obstacle to the realization of the NO-CO reaction by transition metal catalysts in industrial flue gas.

The active components of noble metal and transition metal catalysts for NO reduction by CO have been widely studied. However, the inhibition of O_2 and the limitation of low-temperature activity cannot be avoided. In the future, it is necessary to improve the low-temperature activity and N_2 selectivity of the catalyst under O_2-enriched conditions.

Funding information This work was supported by the National Key R&D Program of China (No. 2017YFC0212500) and the National Natural Science Foundation of China (No. U1810209).

References

Araya P, Gracia F, Jn C, Wolf EE (2002) FTIR study of the reduction reaction of NO by CO over Rh/SiO2 catalysts with different crystallite size. Appl Catal B Environ 38:77–90. https://doi.org/10.1016/s0926-3373(02)00019-x

Araya P, Weissmann C (2000) FTIR study of the oxidation reaction of CO with O2 over bimetallic Pd–Rh_SiO2 catalysts in an oxidized state. Catal Lett 68:33–39. https://doi.org/10.1023/a:1019014932471

Baidya T, Bera P, Mukri BD, Parida SK, Kröcher O, Elsener M, Hegde MS (2013) DRIFTS studies on CO and NO adsorption and NO+CO reaction over Pd2+-substituted CeO2 and Ce0.75Sn0.25O2 catalysts. J Catal 303:117–129. https://doi.org/10.1016/j.jcat.2013.03.020

Baidya T, Marimuthu A, Hegde MS, Ravishankar N, Madras G (2007) Higher Catalytic Activity of Nano-Ce1-x-yTixPdyO2-δ Compared to Nano-Ce1-xPdxO2-δ for CO Oxidation and N2O and NO Reduction by CO: role of Oxide Ion Vacancy. J Phys Chem C 111:830–839. https://doi.org/10.1021/jp064565e

Bellido JDA, Assaf EM (2009) Reduction of NO by CO on Cu/ZrO2/Al2O3 catalysts: characterization and catalytic activities. Fuel 88:1673–1679. https://doi.org/10.1016/j.fuel.2009.04.015

Bera P, Patil KC, Jayaram V, Subbanna GN, Hegde MS (2000) Ionic dispersion of Pt and Pd on CeO2 by combustion method: effect of metal–ceria interaction on catalytic activities for NO reduction and CO and hydrocarbon oxidation. J Catal 196:293–301. https://doi.org/10.1006/jcat.2000.3048

Bera P, Priolkar KR, Sarode PR, Hegde MS, Emura S, Kumashiro R, Lalla NP (2002) Structural investigation of combustion synthesized Cu/CeO2 catalysts by EXAFS and other physical techniques: formation of a Ce1-xCuxO2-δ solid solution. Chem Mater 14:3591–3601. https://doi.org/10.1021/cm0201706

Boaro M, Giordano F, Recchia S, Santo VD, Giona M, Trovarelli A (2004) On the mechanism of fast oxygen storage and release in ceria-zirconia model catalysts. Appl Catal B Environ 52:225–237. https://doi.org/10.1016/j.apcatb.2004.03.021

Boccuzzi F, Guglielminotti E, Martra G, Cerrato G (1994) Nitric oxide reduction by CO on Cu/TiO2 catalysts. J Catal 146:449–459. https://doi.org/10.1006/jcat.1994.1082

Boningari T, Pavani SM, Ettireddy PR, Chuang SSC, Smirniotis PG (2018) Mechanistic investigations on NO reduction with CO over Mn/TiO2 catalyst at low temperatures. Molec Catalysis 451:33–42. https://doi.org/10.1016/j.mcat.2017.10.017

Bowker M, Guo Q, Li Y, Joyner RW (1993) Structure sensitivity in CO oxidation over rhodium. Catal Lett 18:119–123. https://doi.org/10.1007/bf00769504

Brackmann R, Toniolo FS, Schmal M (2016) Synthesis and characterization of Fe-doped CeO2 for application in the NO selective catalytic reduction by CO. Top Catal 59:1772–1786. https://doi.org/10.1007/s11244-016-0698-4

Burch R, Millington PJ, Walker AP (1994) Mechanism of the selective reduction of nitrogen monoxide on platinum-based catalysts in the presence of excess oxygen. Appl Catal B Environ 4:65–94. https://doi.org/10.1016/0926-3373(94)00014-x

Campbell CT, White JM (1978) Chemisorption and reactions of nitric oxide on rhodium. Appl Surf Sci 1:347–359. https://doi.org/10.1016/0378-5963(78)90037-5

Chen J, Zhu J, Zhan Y, Lin X, Cai G, Wei K, Zheng Q (2009a) Characterization and catalytic performance of Cu/CeO2 and Cu/MgO-CeO2 catalysts for NO reduction by CO. Appl Catal A Gen 363:208–215. https://doi.org/10.1016/j.apcata.2009.05.017

Chen JF, Zhan YY, Zhu JJ, Chen CQ, Lin XY, Zheng Q (2010a) The synergetic mechanism between copper species and ceria in NO abatement over Cu/CeO2 catalysts. Appl Catal A Gen 377:121–127. https://doi.org/10.1016/j.apcata.2010.01.027

Chen JF, Zhu JJ, Chen CQ, Zhan YY, Cao YN, Lin XY, Zheng Q (2009b) Effect of Mg addition on the physical and catalytic properties of Cu/CeO2 for NO + CO reduction. Catal Lett 130:254–260. https://doi.org/10.1007/s10562-009-9878-1

Chen LF, González G, Wang JA, Noreña LE, Toledo A, Castillo S, Morán-Pineda M (2005) Surfactant-controlled synthesis of Pd/Ce0.6Zr0.4O2 catalyst for NO reduction by CO with excess oxygen. Appl Surf Sci 243:319–328. https://doi.org/10.1016/j.apsusc.2004.09.074

Chen W, Shen Q, Bartynski RA, Kaghazchi P, Jacob T (2010b) Reduction of NO by CO on unsupported Ir: bridging the materials gap. Chemphyschem 11:2515–2520. https://doi.org/10.1002/cphc.201000254

Chen YN et al (2013) Ternary composite oxide catalysts CuO/Co3O4–CeO2 with wide temperature-window for the preferential oxidation of CO in H2-rich stream. Chem Eng J 234:88–98. https://doi.org/10.1016/j.cej.2013.08.063

Cheng XX, Cheng YR, Wang ZQ, Ma CY (2018) Comparative study of coal based catalysts for NO adsorption and NO reduction by CO. Fuel 214:230–241. https://doi.org/10.1016/j.fuel.2017.11.009

Cheng XX, Wang LY, Wang ZQ, Zhang MZ, Ma CY (2016a) Catalytic performance of NO reduction by CO over activated semicoke supported Fe/Co catalysts. Ind Eng Chem Res 55:12710–12722. https://doi.org/10.1021/acs.iecr.6b00804

Cheng XX, Zhang M, Sun PL, Wang LY, Wang ZQ, Ma CY (2016b) Nitrogen oxides reduction by carbon monoxide over semi-coke supported catalysts in a simulated rotary reactor: reaction performance under dry conditions. Green Chem 18:5305–5324. https://doi.org/10.1039/c6gc01168c

Cheng XX, Zhang XY, Zhang M, Sun PL, Wang ZQ, Ma CY (2017) A simulated rotary reactor for NOx reduction by carbon monoxide over Fe/ZSM-5 catalysts. Chem Eng J 307:24–40. https://doi.org/10.1016/j.cej.2016.08.076

Chin AA, Bell AT (1983) Kinetics of nitric oxide decomposition on silica-supported rhodium. J Phys Chem 87:3700–3706. https://doi.org/10.1021/j100242a025

Cho BK (1994) Mechanistic importance of intermediate N2O + CO reaction in overall NO + CO reaction system. J Catal 148:697–708. https://doi.org/10.1006/jcat.1994.1256

Cho BK, Shanks BH, Bailey JE (1989) Kinetics of NO reduction by CO over supported rhodium catalysts: isotopic cycling experiments. J Catal 115:486–499. https://doi.org/10.1016/0021-9517(89)90052-3

Chuang SSC, Krishnamurthy R, Tan C-D (1995) Reactivity of adsorbed CO toward C2H4, H2, and NO on the surface of supported rhodium catalysts. Colloids Surf A Physicochem Eng Asp 105:35–46. https://doi.org/10.1016/0927-7757(95)03312-7

Chuang SSC, Tan CD (1998) Mechanistic studies of the NO–CO reaction onRh/Al2O3 under net-oxidizing conditions. J Catal 173:95–104. https://doi.org/10.1006/jcat.1997.1922

Ciuparu D, Bensalem A, Pfefferle L (2000) Pd–Ce interactions and adsorption properties of palladium: CO and NO TPD studies over Pd–Ce/Al2O3 catalysts. Appl Catal B Environ 26:241–255. https://doi.org/10.1016/s0926-3373(00)00130-2

Damma D, Boningari T, Ettireddy PR, Reddy BM, Smirniotis PG (2018) Direct decomposition of NOx over TiO2 supported transition metal oxides at low temperatures. Ind Eng Chem Res 57:16615–16621. https://doi.org/10.1021/acs.iecr.8b03532

Damma D, Ettireddy PR, Reddy BM, Smirniotis PG (2019) A review of low temperature NH3-SCR for removal of NOx. Catalysts 9. https://doi.org/10.3390/catal9040349

Deng C et al (2015) NO reduction by CO over CuO supported on CeO2-doped TiO2: the effect of the amount of a few CeO2. Phys Chem Chem Phys 17:16092–16109. https://doi.org/10.1039/c5cp00745c

Deng CS et al (2016) Influences of doping and thermal stability on the catalytic performance of CuO/Ce20M1Ox (M = Zr, Cr, Mn, Fe, Co, Sn) catalysts for NO reduction by CO. RSC Adv 6:113630–113647. https://doi.org/10.1039/c6ra21740k

Ding ZX, Yang HY, Liu JF, Dai WX, Chen X, Wang XX, Fu XZ (2011) Promoted CO oxidation activity in the presence and absence of hydrogen over the TiO2-supported Pt/Co–B bicomponent catalyst. Appl Catal B Environ 101:326–332. https://doi.org/10.1016/j.apcatb.2010.10.001

Dong LH et al (2014) Influence of CeO2 modification on the properties of Fe2O3–Ti0.5Sn0.5O2 catalyst for NO reduction by CO. Catal Sci Technol 4:482–493. https://doi.org/10.1039/c3cy00703k

Dong LH et al (2011) Study of the properties of CuO/VOx/Ti0.5Sn0.5O2 catalysts and their activities in NO + CO reaction. ACS Catal 1:468–480. https://doi.org/10.1021/cs200045f

Fan C, Xiao WD (2013) Origin of site preference of CO and NO adsorption on Pd(111) at different coverages: a density functional theory study. Comput Theore Chem 1004:22–30. https://doi.org/10.1016/j.comptc.2012.10.027

Fernández-García M, Iglesias-Juez A, Martínez-Arias A, Hungría AB, Anderson JA, Conesa JC, Soria J (2004) Role of the state of the metal component on the light-off performance of Pd-based three-way catalysts. J Catal 221:594–600. https://doi.org/10.1016/j.jcat.2003.09.022

Fink T, Dath JP, Imbihl R, Ertl G (1991) Kinetic oscillations in the NO + CO reaction on Pt(100): experiments and mathematical modeling. J Chem Phys 95:2109–2126. https://doi.org/10.1063/1.461010

Fu Y, Tian Y, Lin P (1991) A low-temperature IR spectroscopic study of selective adsorption of NO and CO on CuO/gamma-Al2O3. J Catal 132:85–91. https://doi.org/10.1016/0021-9517(91)90249-4

Fujitani T, Nakamura I, Kobayashi Y, Takahashi A, Haneda M, Hamada H (2007) Adsorption and reactivity of SO2 on Ir(111) and Rh(111). Surf Sci 601:1615–1622. https://doi.org/10.1016/j.susc.2007.01.034

Gaspar AB, Dieguez LC (2000) Dispersion stability and methylcyclopentane hydrogenolysis in Pd/Al2O3 catalysts. Appl Catal A Gen 201:241–251. https://doi.org/10.1016/s0926-860x(00)00442-7

Gayen A, Baidya T, Ramesh GS, Srihari R, Hegde MS (2006) Design and fabrication of an automated temperature programmed reaction system to evaluate 3-way catalysts Ce1−x−y,(La/Y)xPtyO2−δ. J Chem Sci 118:47–55. https://doi.org/10.1007/bf02708765

Ge CY et al (2014) Improving the dispersion of CeO2 on γ-Al2O3 to enhance the catalytic performances of CuO/CeO2/γ-Al2O3 catalysts for NO removal by CO. Catal Commun 51:95–99. https://doi.org/10.1016/j.catcom.2014.03.032

Gholami Z, Luo GH (2018) Low-temperature selective catalytic reduction of NO by CO in the presence of O2 over Cu:Ce catalysts supported by multiwalled carbon nanotubes. Ind Eng Chem Res 57:8871–8883. https://doi.org/10.1021/acs.iecr.8b01343

Goodman DW, Peden CHF, Fisher GB, Oh SH (1993) Comment on structure sensitivity in CO oxidation over rhodium by M. Bowker, Q. Guo, Y. Li and R. W. Joyner. Catal Lett 22:271–274. https://doi.org/10.1007/bf00810373

Graham GW, Logan AD, Shelef M (1993) Oxidation of carbon monoxide by oxygen, nitric oxide and mixtures of O2 and NO over palladium(100). J Phys Chem 97:5445–5446. https://doi.org/10.1021/j100123a001

Granger P, Dathy C, Lecomte JJ, Leclercq L, Prigent M, Mabilon G, Leclercq G (1998a) Kinetics of the NO and CO reaction over platinum catalysts. J Catal 173:304–314. https://doi.org/10.1006/jcat.1997.1932

Granger P, Delannoy L, Lecomte JJ, Dathy C, Praliaud H, Leclercq L, Leclercq G (2002) Kinetics of the CO+NO reaction over bimetallic platinum–rhodium on alumina: effect of ceria incorporation into noble metals. J Catal 207:202–212. https://doi.org/10.1006/jcat.2002.3519

Granger P, Lecomte JJ, Dathy C, Leclercq L, Leclercq G (1998b) Kinetics of the CO+NO reaction over rhodium and platinum–rhodium on alumina. J Catal 175:194–203. https://doi.org/10.1006/jcat.1998.2014

Grzybek T, Rogóż M, Papp H (2004) The interaction of NO with active carbons promoted with transition metal oxides/hydroxides. Catal Today 90:61–68. https://doi.org/10.1016/j.cattod.2004.04.009

Gu XR, Li H, Liu LC, Tang CJ, Gao F, Dong L (2014) Promotional effect of CO pretreatment on CuO/CeO2 catalyst for catalytic reduction of NO by CO. J Rare Earths 32:139–145. https://doi.org/10.1016/s1002-0721(14)60043-0

Guerrero S, Guzmán I, Aguila G, Chornik B, Araya P (2012) Study of Na/Cu/TiO2 catalysts for the storage and reduction of NO. Appl Catal B Environ 123-124:282–295. https://doi.org/10.1016/j.apcatb.2012.04.036

Hailstone RK, DiFrancesco AG, Leong JG, Allston TD, Reed KJ (2009) A study of lattice expansion in CeO2 nanoparticles by transmission electron microscopy. J Phys Chem C 113:15155–15159. https://doi.org/10.1021/jp903468m

Hamada H, Haneda M (2012) A review of selective catalytic reduction of nitrogen oxides with hydrogen and carbon monoxide. Appl Catal A Gen 421-422:1–13. https://doi.org/10.1016/j.apcata.2012.02.005

Haneda M, Fujitani T, Hamada H (2006a) Effect of iridium dispersion on the catalytic activity of Ir/SiO2 for the selective reduction of NO with CO in the presence of O2 and SO2. J Mol Catal A Chem 256:143–148. https://doi.org/10.1016/j.molcata.2006.04.058

Haneda M, Hamada H (2008) Promoting effect of coexisting H2O on the activity of Ir/WO3/SiO2 catalyst for the selective reduction of NO with CO. Chem Lett 37:830–831. https://doi.org/10.1246/cl.2008.830

Haneda M, Hamada H (2010) Promotional role of H2O in the selective catalytic reduction of NO with CO over Ir/WO3/SiO2 catalyst. J Catal 273:39–49. https://doi.org/10.1016/j.jcat.2010.04.021

Haneda M, Kudo H, Nagao Y, Fujitani T, Hamada H (2006b) Enhanced activity of Ba-doped Ir/SiO2 catalyst for NO reduction with CO in the presence of O2 and SO2. Catal Commun 7:423–426. https://doi.org/10.1016/j.catcom.2005.12.020

Haneda M, Pusparatu KY, Nakamura I, Sasaki M, Fujitani T, Hamada H (2005) Promotional effect of SO2 on the activity of Ir/SiO2 for NO reduction with CO under oxygen-rich conditions. J Catal 229:197–205. https://doi.org/10.1016/j.jcat.2004.10.022

Haneda M, Yoshinari T, Sato K, Kintaichi Y, Hamada H (2003) Ir/SiO2 as a highly active catalyst for the selective reduction of NO with CO in the presence of O2 and SO2. Chem Commun. https://doi.org/10.1039/b309981d

He H, Liu M, Dai HX, Qiu WG, Zi XH (2007) An investigation of NO/CO reaction over perovskite-type oxide La0.8Ce0.2B0.4Mn0.6O3 (B=Cu or Ag) catalysts synthesized by reverse microemulsion. Catal Today 126:290–295. https://doi.org/10.1016/j.cattod.2007.06.004

Hecker WC, Bell AT (1983) Reduction of NO by CO over silica-supported rhodium: infrared and kinetic studies. J Catal 84:200–215. https://doi.org/10.1016/0021-9517(83)90098-2

Hecker WC, Bell AT (1984) Infrared observations of Rh-NCO and Si-NCO species formed during the reduction of NO by CO over silica-supported rhodium. J Catal 85:389–397. https://doi.org/10.1016/0021-9517(84)90228-8

Holles JH, Davis RJ, Murray TM, Howe JM (2000) Effects of Pd particle size and ceria loading on NO reduction with CO. J Catal 195:193–206. https://doi.org/10.1006/jcat.2000.2985

Hornung A, Muhler M, Ertl G (1998) The reduction of NO with H2 over Ru/MgO. Catal Lett 53:77–81. https://doi.org/10.1023/a:1019072915187

Hu YH, Dong L, Shen MM, Liu D, Wang J, Ding WP, Chen Y (2001) Influence of supports on the activities of copper oxide species in the low-temperature NO+CO reaction. Appl Catal B Environ 31:61–69. https://doi.org/10.1016/s0926-3373(00)00269-1

Hu Z, Allen FM, Wan CZ, Heck RM, Steger JJ, Lakis RE, Lyman CE (1998) Performance and structure of Pt–Rh three-way catalysts: mechanism for Pt/Rh synergism. J Catal 174:13–21. https://doi.org/10.1006/jcat.1997.1954

Huang SJ, Walters AB, Vannice MA (2000) Adsorption and decomposition of NO on lanthanum oxide. J Catal 192:29–47. https://doi.org/10.1006/jcat.2000.2846

Hungria A, Browning N, Erni R, Fernandezgarcia M, Conesa J, Perezomil J, Martinezarias A (2005a) The effect of Ni in Pd–Ni/(Ce,Zr)O/Al2O3 catalysts used for stoichiometric CO and NO elimination. Part 1: nanoscopic characterization of the catalysts. J Catal 235:251–261. https://doi.org/10.1016/j.jcat.2005.08.011

Hungria A, Fernandezgarcia M, Anderson J, Martinezarias A (2005b) The effect of Ni in Pd–Ni/(Ce,Zr)O/Al2O3 catalysts used for stoichiometric CO and NO elimination. Part 2: catalytic activity and in situ spectroscopic studies. J Catal 235:262–271. https://doi.org/10.1016/j.jcat.2005.08.012

Iglesias-Juez A, Kubacka A, Fernandez-Garcia M, Di Michiel M, Newton MA (2011) Nanoparticulate Pd supported catalysts: size-dependent formation of Pd(I)/Pd(0) and their role in CO elimination. J Am Chem Soc 133:4484–4489. https://doi.org/10.1021/ja110320y

Iglesias-Juez A, Martínez-Arias A, Fernández-García M (2004) Metal–promoter interface in Pd/(Ce,Zr)Ox/Al2O3 catalysts: effect of thermal aging. J Catal 221:148–161. https://doi.org/10.1016/j.jcat.2003.07.010

Ilieva L et al (2015) NO reduction by CO over gold catalysts supported on Fe-loaded ceria. Appl Catal B Environ 174-175:176–184. https://doi.org/10.1016/j.apcatb.2015.03.004

Iliopoulou EF, Efthimiadis EA, Lappas AA, Vasalos IA (2005a) Effect of Ru-based catalytic additives on NO and CO formed during regeneration of spent FCC catalyst. Ind Eng Chem Res 44:4922–4930. https://doi.org/10.1021/ie049192n

Iliopoulou EF, Efthimiadis EA, Nalbandian L, Vasalos IA, Barth JO, Lercher JA (2005b) Ir-based additives for NO reduction and CO oxidation in the FCC regenerator: evaluation, characterization and mechanistic studies. Appl Catal B Environ 60:277–288. https://doi.org/10.1016/j.apcatb.2005.03.011

Iliopoulou EF, Evdou AP, Lemonidou AA, Vasalos IA (2004) Ag/alumina catalysts for the selective catalytic reduction of NOx using various reductants. Appl Catal A Gen 274:179–189. https://doi.org/10.1016/j.apcata.2004.06.052

Illas F, López N, Ricart JM, Clotet A, Conesa JC, Fernández-García M (1998) Interaction of CO and NO with PdCu(111) Surfaces. J Phys Chem B 102:8017–8023. https://doi.org/10.1021/jp982118w

Inomata H, Shimokawabe M, Arai M (2007) An Ir/WO3 catalyst for selective reduction of NO with CO in the presence of O2 and/or SO2. Appl Catal A Gen 332:146–152. https://doi.org/10.1016/j.apcata.2007.08.013

Iojoiu E, Gélin P, Praliaud H, Primet M (2004) Reduction of NO by propene over supported iridium catalysts under lean-burn conditions: an in situ FTIR study. Appl Catal A Gen 263:39–48. https://doi.org/10.1016/j.apcata.2003.11.038

Iwamoto M, Yahiro H, Mine Y, Kagawa S (1989) Excessively copper ion-exchanged ZSM-5 Zeolites as highly active catalysts for direct decomposition of nitrogen monoxide. Chem Lett 18:213–216. https://doi.org/10.1246/cl.1989.213

Iwamoto M, Yahiro H, Torikai Y, Yoshioka T, Mizuno N (1990) Novel preparation method of highly copper ion-exchanged ZSM-5 zeolites and their catalytic activities for NO decomposition. Chem Lett 19:1967–1970. https://doi.org/10.1246/cl.1990.1967

Jiang XY, Ding GH, Lou LP, Chen YX, Zheng XM (2004) Effect of ZrO2 addition on CuO/TiO2 activity in the NO+CO reaction. Catal Today 93-95:811–818. https://doi.org/10.1016/j.cattod.2004.06.074

K.Cho B (1992) Mechanistic importance of intermediate N2O+CO reaction in overall NO+CO reaction system. J Catal 138:255–266. https://doi.org/10.1016/0021-9517(92)90021-9

Kacimi M, Ziyad M, Liotta LF (2015) Cu on amorphous AlPO4: preparation, characterization and catalytic activity in NO reduction by CO in presence of oxygen. Catal Today 241:151–158. https://doi.org/10.1016/j.cattod.2014.04.003

Kobylinski TP, Taylor BW (1974) The catalytic chemistry of nitric oxide. J Catal 33:376–384. https://doi.org/10.1016/0021-9517(74)90284-x

Komvokis VG, Marti M, Delimitis A, Vasalos IA, Triantafyllidis KS (2011) Catalytic decomposition of N2O over highly active supported Ru nanoparticles (≤3nm) prepared by chemical reduction with ethylene glycol. Appl Catal B Environ 103:62–71. https://doi.org/10.1016/j.apcatb.2011.01.009

Koopman PGJ, Kieboom APG, Bekkum HV (1981) Characterization of ruthenium catalysts as studied by temperature programmed reduction. J Catal 69:172–179. https://doi.org/10.1016/0021-9517(81)90139-1

Kotsifa A, Kondarides D, Verykios X (2008) A comparative study of the selective catalytic reduction of NO by propylene over supported Pt and Rh catalysts. Appl Catal B Environ 80:260–270. https://doi.org/10.1016/j.apcatb.2007.11.037

Krishnamurthy R, Chuang SSC (1995) Pulse reaction studies of transient nature of adsorbates during NO-CO reaction over Rh/SiO2. J Phys Chem 99:16727–16735. https://doi.org/10.1021/j100045a037

Krishnamurthy R, Chuang SSC, Balakos MW (1995) Step and pulse transient studies of Ir-observable adsorbates during NO and CO reaction on Rh/SiO2. J Catal 157:512–522. https://doi.org/10.1006/jcat.1995.1315

Labhsetwar N et al (2007) Catalytic properties of Ru-mordenite for NO reduction. J Mol Catal A Chem 261:213–217. https://doi.org/10.1016/j.molcata.2006.08.013

Lei GD, Kevan L (1991) Characterization of ruthenium species generated in H-X zeolite: interaction with carbon monoxide, nitric oxide, oxygen, and water. J Phys Chem 95:4506–4514. https://doi.org/10.1021/j100164a061

Li D et al (2011a) The remarkable enhancement of CO-pretreated CuO-Mn2O3/γ-Al2O3 supported catalyst for the reduction of NO with CO: the formation of surface synergetic oxygen vacancy. Chem Eur J 17:5668–5679. https://doi.org/10.1002/chem.201002786

Li GH, Liu C, Rao MJ, Fan ZY, You ZX, Zhang YB, Jiang T (2014a) Behavior of SO2 in the process of flue gas circulation sintering (FGCS) for iron ores. ISIJ Int 54:37–42. https://doi.org/10.2355/isijinternational.54.37

Li HY, Zhang SL, Zhong Q (2013) Effect of nitrogen doping on oxygen vacancies of titanium dioxide supported vanadium pentoxide for ammonia-SCR reaction at low temperature. J Colloid Interface Sci 402:190–195. https://doi.org/10.1016/j.jcis.2012.10.033

Li J, Luo GH, Chu Y, Wei F (2012) Experimental and modeling analysis of NO reduction by CO for a FCC regeneration process. Chem Eng J 184:168–175. https://doi.org/10.1016/j.cej.2012.01.024

Li J, Luo GH, Wei F (2011b) A multistage NOx reduction process for a FCC regenerator. Chem Eng J 173:296–302. https://doi.org/10.1016/j.cej.2011.06.070

Li J, Wang S, Zhou L, Luo GH, Wei F (2014b) NO reduction by CO over a Fe-based catalyst in FCC regenerator conditions. Chem Eng J 255:126–133. https://doi.org/10.1016/j.cej.2014.06.015

Li LD, Yu JJ, Hao ZP, Xu ZP (2007) Novel Ru−Mg−Al−O catalyst derived from hydrotalcite-like compound for NO storage/decomposition/reduction. J Phys Chem C 111:10552–10559. https://doi.org/10.1021/jp0678352

Li YH, Lu GQ, Rudolph V (1998) The kinetics of NO and N2O reduction over coal chars in fluidised-bed combustion. Chem Eng Sci 53:1–26. https://doi.org/10.1016/S0009-2509(97)87569-0

Li YH, Radovic LR, Lu GQ, Rudolph V (1999) A new kinetic model for the NO–carbon reaction. Chem Eng Sci 54:4125–4136. https://doi.org/10.1016/s0009-2509(99)00121-9

Liu KJ, Yu QB, Liu JL, Wang K, Han ZC, Xuan YN, Qin Q (2017) Selection of catalytically active elements for removing NO and CO from flue gas at low temperatures. New J Chem 41:13993–13999. https://doi.org/10.1039/c7nj02694c

Liu LJ et al (2010) Influence of supports structure on the activity and adsorption behavior of copper-based catalysts for NO reduction. J Mol Catal A Chem 327:1–11. https://doi.org/10.1016/j.molcata.2010.05.002

López T, Hernandez-Ventura J, Asomoza M, Campero A, Gómez R (1999) Support effect on Cu–Ru/SiO2 sol–gel catalysts. Mater Lett 41:309–316. https://doi.org/10.1016/s0167-577x(99)00148-2

Luo M, Ma J, Lu J, Song Y, Wang Y (2007) High-surface area CuO–CeO2 catalysts prepared by a surfactant-templated method for low-temperature CO oxidation. J Catal 246:52–59. https://doi.org/10.1016/j.jcat.2006.11.021

Lv Y et al (2013) Investigation of surface synergetic oxygen vacancy in CuO-CoO binary metal oxides supported on gamma-Al2O3 for NO removal by CO. J Colloid Interface Sci 390:158–169. https://doi.org/10.1016/j.jcis.2012.08.061

Lv YY et al (2012) Investigation of the physicochemical properties of CuO-CoO binary metal oxides supported on gamma-Al2O3 and their activity for NO removal by CO. J Colloid Interface Sci 372:63–72. https://doi.org/10.1016/j.jcis.2012.01.014

Ma L, Luo M-F, Chen S-Y (2003) Redox behavior and catalytic properties of CuO/Ce0.8Zr0.2O2 catalysts. Appl Catal A Gen 242:151–159. https://doi.org/10.1016/s0926-860x(02)00509-4

Makeev AG, Nieuwenhuys BE (1998) Mathematical modeling of the NO+H2/Pt(100) reaction: "Surface explosion," kinetic oscillations, and chaos. J Chem Phys 108:3740–3749. https://doi.org/10.1063/1.475767

Makeev AG, Peskov NV (2013) The reduction of NO by CO under oxygen-rich conditions in a fixed-bed catalytic reactor: a mathematical model that can explain the peculiar behavior. Appl Catal B Environ 132-133:151–161. https://doi.org/10.1016/j.apcatb.2012.11.025

Martínez-Arias A, Hungría AB, Fernández-García M, Iglesias-Juez A, Anderson JA, Conesa JC (2004) Light-off behaviour of PdO/γ-Al2O3 catalysts for stoichiometric CO–O2 and CO–O2–NO reactions: a combined catalytic activity–in situ DRIFTS study. J Catal 221:85–92. https://doi.org/10.1016/s0021-9517(03)00277-x

Martínez-Arias A et al (2012) Redox and catalytic properties of CuO/CeO2 under CO+O2+NO: promoting effect of NO on CO oxidation. Catal Today 180:81–87. https://doi.org/10.1016/j.cattod.2011.02.014

Mccabe RW, Wong C (1990) Steady-state kinetics of the CO-N2O reaction over an alumina-supported rhodium catalyst. J Catal 121:422–431. https://doi.org/10.1016/0021-9517(90)90250-N

Mehandjiev D, Bekyarova E (1994) Catalytic neutralization of NO on a carbon-supported cobalt oxide catalyst. J Colloid Interface Sci 166:476–480. https://doi.org/10.1006/jcis.1994.1320

Mergler YJ, van Aalst A, van Delft J, Nieuwenhuys BE (1996) CO oxidation over promoted Pt catalysts. Appl Catal B Environ 10:245–261. https://doi.org/10.1016/s0926-3373(96)00017-3

Ming M, Yan LP, Lu FY (1997) The catalytic removal of CO and NO over Co^Pt (Pd, Rh)Al2O3 catalysts and their structural characterizations. Catal Lett 48:213–222. https://doi.org/10.1023/a:1019099625781

Muraki H, Fujitani Y (1986) Nitric oxide reduction by carbon monoxide over noble-metal catalysts under cycled feedstreams. Ind Eng Chem Prod Res Dev 25:414–419. https://doi.org/10.1021/i300023a008

Nakatsuji T, Yamaguchi T, Sato N, Ohno H (2008) A selective NOx reduction on Rh-based catalysts in lean conditions using CO as a main reductant. Appl Catal B Environ 85:61–70. https://doi.org/10.1016/j.apcatb.2008.06.024

Nawdali M, Iojoiu E, Gélin P, Praliaud H, Primet M (2001a) Influence of the pre-treatment on the structure and reactivity of Ir/γ-Al2O3 catalysts in the selective reduction of nitric oxide by propene. Appl Catal A Gen 220:129–139. https://doi.org/10.1016/s0926-860x(01)00723-2

Nawdali M, Praliaud H, Primet M (2001b) SCR of NO over Ir/Al2O3 catalysts. Importance of the activation procedure and influence of the dispersion. Top Catal 16(17):199–204. https://doi.org/10.1023/a:1016619906586

Neyertz C, Volpe M (1998) Preparation of binary palladium-vanadium supported catalysts from metal acetylacetonates. Colloids Surf A Physicochem Eng Asp 136:63–69. https://doi.org/10.1016/s0927-7757(97)00249-5

Noronha FB, Baldanza MAS, Schmal M (1999) CO and NO adsorption on alumina–Pd–Mo catalysts: effect of the precursor salts. J Catal 188:270–280. https://doi.org/10.1006/jcat.1999.2644

Novakova J, Kubelkova L (1997) Contribution to the mechanism of NO reduction by CO over Pt/NaX zeolite. Appl Catal B Environ 14:273–286. https://doi.org/10.1016/s0926-3373(97)00029-5

Ogura M, Kawamura A, Matsukata M, Kikuchi E (2000) Catalytic activity of Ir for NO-CO reaction in the presence of SO2 and excess oxygen. Chem Lett 29:146–147. https://doi.org/10.1246/cl.2000.146

Oh S (1986) Comparative kinetic studies of CO$z.sbnd;O2 and CO$z.sbnd;NO reactions over single crystal and supported rhodium catalysts. J Catal 100:360–376. https://doi.org/10.1016/0021-9517(86)90103-x

Oh SH, Carpenter JE (1986) Platinum-rhodium synergism in three-way automotive catalysts. J Catal 98:178–190. https://doi.org/10.1016/0021-9517(86)90307-6

Oh SH, Fisher GB, Carpenter JE, Goodmant DW (1986) Comparative kinetic studies of CO+O2 and CO+NO reactions over single crystal and supported rhodium catalysts. J Catal 100:360–376. https://doi.org/10.1016/0021-9517(86)90103-x

Ohyama J, Ishikawa H, Mahara Y, Nishiyama T, Satsuma A (2016) Formation of Ru shell on Co/Al2O3 by galvanic deposition method and its high catalytic performance for three-way conversion. Bull Chem Soc Jpn 89:914–921. https://doi.org/10.1246/bcsj.20160102

Okamoto Y, Gotoh H (1997) Copper-zirconia catalysts for NO+CO reactions. Catal Today 36:71–79. https://doi.org/10.1016/s0920-5861(96)00198-8

Patel A, Shukla P, Rufford T, Wang S, Chen J, Rudolph V, Zhu Z (2011) Catalytic reduction of NO by CO over copper-oxide supported

mesoporous silica. Appl Catal A Gen 409-410:55–65. https://doi.org/10.1016/j.apcata.2011.09.024
Patel A, Shukla P, Rufford TE, Rudolph V, Zhu ZH (2014) Selective catalytic reduction of NO with CO using different metal-oxides incorporated in MCM-41. Chem Eng J 255:437–444. https://doi.org/10.1016/j.cej.2014.06.032
Paul DK, Ballinger TH, Yates JT (1990) Rhodium surface chemistry on a chemically modified alumina support. J Phys Chem 94:4617–4622. https://doi.org/10.1021/j100374a046
Paul DK, Yates JT (1991) Protection of a rhodium/alumina catalyst under extreme environmental conditions. J Phys Chem 95:1699–1703. https://doi.org/10.1021/j100157a040
Peden CHF, Goodman DW, Blair DS, Berlowitz PJ, Fisher GB, Oh SH (1988) Kinetics of carbon monoxide oxidation by oxygen or nitric oxide on rhodium(111) and rhodium(100) single crystals. J Phys Chem 92:1563–1567. https://doi.org/10.1021/j100317a038
Pirug G (1977) A low-pressure study of the reduction of NO by H2 on polycrystalline platinum. J Catal 50:64–76. https://doi.org/10.1016/0021-9517(77)90009-4
Pirugand G, Bonzel HP (1977) A low-pressure study of the reduction of NO by H2 on polycrystalline platinum. J Catal 50:64–76. https://doi.org/10.1016/0021-9517(77)90009-4
Qin YH, Huang L, Zheng JX, Ren Q (2016) Low-temperature selective catalytic reduction of NO with CO over A-Cu-BTC and AOx/CuOy/C catalyst. Inorg Chem Commun 72:78–82. https://doi.org/10.1016/j.inoche.2016.08.018
Rainer DR, Koranne M, Vesecky SM, Goodman DW (1997) CO + O2and CO + NO Reactions over Pd/Al2O3 Catalysts. J Phys Chem B 101:10769–10774. https://doi.org/10.1021/jp971262z
Rasko J (1981) Infrared study of the formation and stability of isocyanate species on some unsupported noble metals. J Catal 71:219–222. https://doi.org/10.1016/0021-9517(81)90220-7
Reddy BV, Khanna SN (2004) Self-stimulated NO reduction and CO oxidation by iron oxide clusters. Phys Rev Lett 93:068301. https://doi.org/10.1103/PhysRevLett.93.068301
Rosas JM, Rodríguez-Mirasol J, Ts C (2010) NO reduction on carbon-supported chromium catalysts†. Energy Fuel 24:3321–3328. https://doi.org/10.1021/ef901455v
Rosas JM, Ruiz-Rosas R, Rodríguez-Mirasol J, Cordero T (2012) Kinetic study of NO reduction on carbon-supported chromium catalysts. Catal Today 187:201–211. https://doi.org/10.1016/j.cattod.2011.10.032
Roy S, Hegde MS (2008) Pd ion substituted CeO2: a superior de-NOx catalyst to Pt or Rh metal ion doped ceria. Catal Commun 9:811–815. https://doi.org/10.1016/j.catcom.2007.09.019
Roy S, Marimuthu A, Hegde MS, Madras G (2007a) High rates of CO and hydrocarbon oxidation and NO reduction by CO over Ti0.99Pd0.01O1.99. Appl Catal B Environ 73:300–310. https://doi.org/10.1016/j.apcatb.2007.01.003
Roy S, Marimuthu A, Hegde MS, Madras G (2007b) High rates of NO and N2O reduction by CO, CO and hydrocarbon oxidation by O2 over nano crystalline Ce0.98Pd0.02O2−δ: catalytic and kinetic studies. Appl Catal B Environ 71:23–31. https://doi.org/10.1016/j.apcatb.2006.08.005
S.J.Tauster LLM (1976) The NO-CO reaction in the presence of excess O2 as catalyzed by iridium. J Catal 41:192–195. https://doi.org/10.1016/0021-9517(76)90216-5
Salker AV, Desai MSF (2016) Catalytic activity and mechanistic approach of NO reduction by CO over M0.05Co2.95O4 (M=Rh, Pd&Ru) spinel system. Appl Surf Sci 389:344–353. https://doi.org/10.1016/j.apsusc.2016.07.121
Schmal M, Baldanza MAS, Vannice MA (1999) Pd-xMo/Al2O3 catalysts for NO reduction by CO. J Catal 185:138–151. https://doi.org/10.1006/jcat.1999.2465
Schwartz SB, Schmidt LD, Fisher GB (1986) Carbon monoxide + oxygen reaction on rhodium (III): steady-state rates and adsorbate coverages. J Phys Chem 90:6194–6200. https://doi.org/10.1021/j100281a027
Senanayake SD et al (2016) Interfacial Cu+ promoted surface reactivity: carbon monoxide oxidation reaction over polycrystalline copper–titania catalysts. Surf Sci 652:206–212. https://doi.org/10.1016/j.susc.2016.02.014
Shangguan WF, Teraoka Y, Kagawa S (1996) Simultaneous catalytic removal of NO and diesel soot particulates over ternary ABO spineltype oxides. Appl Catal B Environ 8:217–227. https://doi.org/10.1016/0926-3373(95)00070-4
Shelef M, Graham GW (2006) Why rhodium in automotive three-way catalysts? Catal Rev 36:433–457. https://doi.org/10.1080/01614949408009468
Shi C, Cheng MJ, Qu ZP, Yang XF, Bao XH (2002) On the selectively catalytic reduction of NOx with methane over Ag-ZSM-5 catalysts. Appl Catal B Environ 36:173–182. https://doi.org/10.1016/s0926-3373(01)00234-x
Shimokawabe M, Niitsu M, Inomata H, Iwasa N, Arai M (2005) A highly active Ir/WO3 catalyst for the selective reduction of NO by CO in the presence of O2 or O2+ SO2. Chem Lett 34:1426–1427. https://doi.org/10.1246/cl.2005.1426
Shimokawabe M, Umeda N (2004) Selective catalytic reduction of NO by CO over supported iridium and rhodium catalysts. Chem Lett 33:534–535. https://doi.org/10.1246/cl.2004.534
Shin HU, Lolla D, Nikolov Z, Chase GG (2016) Pd–Au nanoparticles supported by TiO2 fibers for catalytic NO decomposition by CO. J Ind Eng Chem 33:91–98. https://doi.org/10.1016/j.jiec.2015.09.020
Sierra-Pereira CA, Urquieta-González EA (2014) Reduction of NO with CO on CuO or Fe2O3 catalysts supported on TiO2 in the presence of O2, SO2 and water steam. Fuel 118:137–147. https://doi.org/10.1016/j.fuel.2013.10.054
Simonot L, Fo G, Maire G (1997) A comparative study of LaCoO3, CO3O4 and a mix of LaCoO3—Co3O4. Appl Catal B Environ 11:181–191. https://doi.org/10.1016/s0926-3373(96)00047-1
Solymosi F, Bansagi T (1995) Infrared spectroscopic study of the isocyanate surface complex over Cu-ZSM-5 catalysts. J Catal 156:75–84. https://doi.org/10.1006/jcat.1995.1233
Song Y-J, Jesús YML-D, Fanson PT, Williams CT (2014) Kinetic evaluation of direct NO decomposition and NO–CO reaction over dendrimer-derived bimetallic Ir–Au/Al2O3 catalysts. Appl Catal B Environ 154-155:62–72. https://doi.org/10.1016/j.apcatb.2014.01.065
Song Y-J, López-De Jesús YM, Fanson PT, Williams CT (2013) Preparation and characterization of dendrimer-derived bimetallic Ir–Au/Al2O3 catalysts for CO oxidation. J Phys Chem C 117:10999–11007. https://doi.org/10.1021/jp310511q
Song ZX, Liu W, Nishiguchi H (2007) Quantitative analyses of oxygen release/storage and CO2 adsorption on ceria and Pt–Rh/ceria. Catal Commun 8:725–730. https://doi.org/10.1016/j.catcom.2006.08.048
Sreekanth PM, Smirniotis PG (2007) Selective reduction of NO with CO Over titania supported transition metal oxide catalysts. Catal Lett 122:37–42. https://doi.org/10.1007/s10562-007-9365-5
Stegenga S, van Soest R, Kapteijn F, Moulijn JA (1993) Nitric oxide reduction and carbon monoxide oxidation over carbon-supported copper-chromium catalysts. Appl Catal B Environ 2:257–275. https://doi.org/10.1016/0926-3373(93)80001-t
Sugi Y, Todo N, Sato T (1975) The catalytic reduction of nitric oxide by carbon monoxide over a Fe2O3 catalyst. Bull Chem Soc Jpn 48:337–338. https://doi.org/10.1246/bcsj.48.337
Sui C, Yuan FL, Zhang ZP, Wang D, Niu XY, Zhu YJ (2017) Catalytic activity of Ru/La1.6Ba0.4NiO4 perovskite-like catalyst for NO+CO reaction: interaction between Ru and La1.6Ba0.4NiO4. Molec Catalysis 437:37–46. https://doi.org/10.1016/j.mcat.2017.05.004
Sun BZ, Chen WK, Xu YJ (2009) Coadsorption of CO and NO on the Cu(2)O(111) surface: a periodic density functional theory study. J Chem Phys 131:174503. https://doi.org/10.1063/1.3251055

Sun CZ, Tang YJ, Gao F, Sun JF, Ma KL, Tang CJ, Dong L (2015) Effects of different manganese precursors as promoters on catalytic performance of CuO-MnOx/TiO2 catalysts for NO removal by CO. Phys Chem Chem Phys 17:15996–16006. https://doi.org/10.1039/c5cp02158h

Sun P, Cheng X, Lai Y, Wang Z, Ma C, Chang J, Zhou P (2019) N-Doped FeCo/ASC catalysts for NOx reduction by CO in a simulated rotary reactor. Catalysis Sci Tech 9:4429–4440. https://doi.org/10.1039/c9cy00786e

Szymański GS, Grzybek T, Papp H (2004) Influence of nitrogen surface functionalities on the catalytic activity of activated carbon in low temperature SCR of NO with NH3. Catal Today 90:51–59. https://doi.org/10.1016/j.cattod.2004.04.008

Takahashi A, Nakamura I, Haneda M, Fujitani T, Hamada H (2006) Role of tungsten in promoting selective reduction of NO with CO over Ir/WO3–SiO2 catalysts. Catal Lett 112:133–138. https://doi.org/10.1007/s10562-006-0192-x

Tamai T, Haneda M, Fujitani T, Hamada H (2007) Promotive effect of Nb2O5 on the catalytic activity of Ir/SiO2 for NO reduction with CO under oxygen-rich conditions. Catal Commun 8:885–888. https://doi.org/10.1016/j.catcom.2006.09.004

Tang CJ, Sun BW, Sun JF, Hong X, Deng Y, Gao F, Dong L (2017) Solid state preparation of NiO-CeO2 catalyst for NO reduction. Catal Today 281:575–582. https://doi.org/10.1016/j.cattod.2016.05.026

Tanikawa K, Egawa C (2011) Effect of barium addition over palladium catalyst for CO–NO–O2 reaction. J Mol Catal A Chem 349:94–99. https://doi.org/10.1016/j.molcata.2011.08.025

Tarjomannejad A, Farzi A, Gómez MJI, Niaei A, Salari D, Albaladejo-Fuentes V (2016) Catalytic reduction of NO by CO over LaMn1−xFexO3 and La0.8A0.2Mn0.3Fe0.7O3 (A = Sr, Cs, Ba, Ce) perovskite catalysts. Catal Lett 146:2330–2340. https://doi.org/10.1007/s10562-016-1860-0

Taylor K (1974) The dual state behavior of supported noble metal catalysts. J Catal 35:34–43. https://doi.org/10.1016/0021-9517(74)90180-8

Taylor KC, Schlatter JC (1980) Selective reduction of nitric oxide over noble metals. J Catal 63:53–71. https://doi.org/10.1016/0021-9517(80)90059-7

Teraoka Y, Nii H, Kagawa S, Jansson K, Nygren M (2000) Influence of the simultaneous substitution of Cu and Ru in the perovskite-type (La,Sr)MO3 (M=Al,Mn,Fe,Co) on the catalytic activity for CO oxidation and CO–NO reactions. Appl Catal A Gen 194-195:35–41. https://doi.org/10.1016/s0926-860x(99)00351-8

Trovarelli Ad C, Dolcetti G (1997) Design better cerium-based oxidation catalysts. Chem Tech 27:32–37

Uchiyama T, Karita R, Nishibori M, Einaga H, Teraoka Y (2015) Preparation and characterization of Pd loaded Sr-deficient K2NiF4-type (La, Sr)2MnO4 catalysts for NO–CO reaction. Catal Today 251:7–13. https://doi.org/10.1016/j.cattod.2014.09.033

Unland ML (1973) Isocyanate intermediates in the reaction nitrogen monoxide + carbon monoxide over a platinum/aluminum oxide catalyst. J Phys Chem 77:1952–1956. https://doi.org/10.1021/j100635a006

Venegas F et al (2019) The transient reduction of NO with CO and naphthalene in the presence of oxygen using a core–shell SmCeO2@TiO2-supported copper catalyst. Catalysis Sci Tech 9:3408–3415. https://doi.org/10.1039/c9cy00545e

Voorhoeve RJH, Trimble LE (1975) Reduction of nitric oxide with carbon monoxide and hydrogen over ruthenium catalysts. J Catal 38:80–91. https://doi.org/10.1016/0021-9517(75)90065-2

Wang AQ, Liang DB, Xu CH, Sun XY, Zhang T (2001) Catalytic reduction of NO over in situ synthesized Ir/ZSM-5 monoliths. Appl Catal B Environ 32:205–212. https://doi.org/10.1016/s0926-3373(01)00138-2

Wang AQ, Ma L, Cong Y, Zhang T, Liang DB (2003) Unique properties of Ir/ZSM-5 catalyst for NO reduction with CO in the presence of excess oxygen. Appl Catal B Environ 40:319–329. https://doi.org/10.1016/s0926-3373(02)00157-1

Wang LY, Cheng XX, Wang ZQ, Ma CY, Qin YK (2017a) Investigation on Fe-Co binary metal oxides supported on activated semi-coke for NO reduction by CO. Appl Catal B Environ 201:636–651. https://doi.org/10.1016/j.apcatb.2016.08.021

Wang LY, Cheng XX, Wang ZQ, Zhang XY, Ma CY (2017b) NO reduction by CO over iron-based catalysts supported by activated semi-coke. Can J Chem Eng 95:449–458. https://doi.org/10.1002/cjce.22678

Wang LY, Wang ZQ, Cheng XX, Zhang MZ, Qin YK, Ma CY (2017c) In situ DRIFTS study of the NO+CO reaction on Fe–Co binary metal oxides over activated semi-coke supports. RSC Adv 7:7695–7710. https://doi.org/10.1039/c6ra26395j

Wang Y, Zhu AM, Zhang YZ, Au CT, Yang XF, Shi C (2008) Catalytic reduction of NO by CO over NiO/CeO2 catalyst in stoichiometric NO/CO and NO/CO/O2 reaction. Appl Catal B Environ 81:141–149. https://doi.org/10.1016/j.apcatb.2007.12.005

Weisweiler W, Hizbullah K, Kureti S (2002) Simultaneous catalytic conversion of NOx and soot from diesel engines exhaust into nitrogen and carbon dioxide. Chem Eng Technol 25:140–143

Wen B, He MY (2002) Study of the Cu-Ce synergism for NO reduction with CO in the presence of O2, H2O and SO2 in FCC operation. Appl Catal B Environ 37:75–82. https://doi.org/10.1016/s0926-3373(01)00316-2

Wögerbauer C, Maciejewski M, Baiker A (2001a) Reduction of nitrogen oxides over unsupported iridium: effect of reducing agent. Appl Catal B Environ 34:11–27. https://doi.org/10.1016/s0926-3373(01)00195-3

Wögerbauer C, Maciejewski M, Baiker A, Göbel U (2001b) Ir/H-ZSM-5 catalysts in the selective reduction of NOx with hydrocarbons. Top Catal 16(17):181–186. https://doi.org/10.1023/a:1016663721607

Wögerbauer C, Maciejewski M, Baiker A, Göbel U (2001c) Structural properties and catalytic behaviour of iridium black in the selective reduction of no by hydrocarbons. J Catal 201:113–127. https://doi.org/10.1006/jcat.2001.3238

Wu LJ, Wiesmann HJ, Moodenbaugh AR, Klie RF, Zhu YM, Welch DO, Suenaga M (2004) Oxidation state and lattice expansion of CeO2−x nanoparticles as a function of particle size. Phys Rev B 69. https://doi.org/10.1103/PhysRevB.69.125415

Xiao P, Davis RC, Ouyang XY, Li JL, Thomas A, Scott SL, Zhu JJ (2014) Mechanism of NO reduction by CO over Pt/SBA-15. Catal Commun 50:69–72. https://doi.org/10.1016/j.catcom.2014.02.027

Xie W, Sun ZC, Xiong YW, Li LT, Wu T, Liang DM (2014) Effects of surface chemical properties of activated coke on selective catalytic reduction of NO with NH3 over commercial coal-based activated coke. Int J Min Sci Technol 24:471–475. https://doi.org/10.1016/j.ijmst.2014.05.009

Xiong Y et al (2014) Effect of CO-pretreatment on the CuO–V2O5/γ-Al2O3 catalyst for NO reduction by CO. Catal Sci Technol 4:4416–4425. https://doi.org/10.1039/c4cy00785a

Xu H, Fu Q, Guo XG, Bao XH (2012) Architecture of Pt?Co bimetallic catalysts for catalytic CO oxidation. ChemCatChem 4:1645–1652. https://doi.org/10.1002/cctc.201200255

Xu XP, Chen PJ, Goodman DW (1994) A comparative study of the coadsorption of carbon monoxide and nitric oxide on Pd(100), Pd(111), and silica-supported palladium particles with infrared reflection-absorption spectroscopy. J Phys Chem 98:9242–9246. https://doi.org/10.1021/j100088a025

Yamamoto T et al (2002) NO reduction with CO in the presence of O2 over Al2O3-supported and Cu-based catalysts. PCCP 4:2449–2458. https://doi.org/10.1039/b201120b

Yang TT, Bi HT, Cheng X (2011) Effects of O2, CO2 and H2O on NOx adsorption and selective catalytic reduction over Fe/ZSM-5. Appl Catal B Environ 102:163–171. https://doi.org/10.1016/j.apcatb.2010.11.038

Yao XJ, Gao F, Cao Y, Tang CJ, Deng Y, Dong L, Chen Y (2013a) Tailoring copper valence states in CuO/gamma-Al2O3 catalysts by an in situ technique induced superior catalytic performance for simultaneous elimination of NO and CO. Phys Chem Chem Phys 15: 14945–14950. https://doi.org/10.1039/c3cp52493k

Yao XJ et al (2016) Preparation, characterization, and catalytic performance of high efficient CeO2-MnOx-Al2O3 catalysts for NO elimination. Chin J Catal 37:1369–1380. https://doi.org/10.1016/s1872-2067(15)61098-1

Yao XJ, Tang CJ, Gao F, Dong L (2014a) Research progress on the catalytic elimination of atmospheric molecular contaminants over supported metal-oxide catalysts. Catal Sci Technol 4. https://doi.org/10.1039/c4cy00397g

Yao XJ et al (2013b) Investigation of the physicochemical properties and catalytic activities of Ce0.67M0.33O2(M = Zr4+, Ti4+, Sn4+) solid solutions for NO removal by CO. Catal Sci Technol 3:688–698. https://doi.org/10.1039/c2cy20610b

Yao XJ et al (2014b) Correlation between the physicochemical properties and catalytic performances of CexSn1–xO2 mixed oxides for NO reduction by CO. Appl Catal B Environ 144:152–165. https://doi.org/10.1016/j.apcatb.2013.06.020

Yao XJ et al (2013c) A comparative study of different doped metal cations on the reduction, adsorption and activity of CuO/Ce0.67M0.33O2 (M=Zr4+, Sn4+, Ti4+) catalysts for NO+CO reaction. Appl Catal B Environ 130-131:293–304. https://doi.org/10.1016/j.apcatb.2012.11.020

Yin L, Wang Y, Pang G, Koltypin Y, Gedanken A (2002) Sonochemical synthesis of cerium oxide nanoparticles-effect of additives and quantum size effect. J Colloid Interface Sci 246:78–84. https://doi.org/10.1006/jcis.2001.8047

Yin SF, Xu BQ, Zhou XP, Au CT (2004) A mini-review on ammonia decomposition catalysts for on-site generation of hydrogen for fuel cell applications. Appl Catal A Gen 277:1–9. https://doi.org/10.1016/j.apcata.2004.09.020

Yoshinari T, Sato K, Haneda M, Kintaichi Y, Hamada H (2001) Remarkable promoting effect of coexisting SO2 on the catalytic activity of Ir/SiO2 for NO reduction in the presence of oxygen. Catal Commun 2:155–158. https://doi.org/10.1016/s1566-7367(01)00025-5

Yoshinari T, Sato K, Haneda M, Kintaichi Y, Hamada H (2003) Positive effect of coexisting SO2 on the activity of supported iridium catalysts for NO reduction in the presence of oxygen. Appl Catal B Environ 41:157–169. https://doi.org/10.1016/s0926-3373(02)00208-4

Yu Q, Yao XJ, Zhang HL, Gao F, Dong L (2012) Effect of ZrO2 addition method on the activity of Al2O3-supported CuO for NO reduction with CO: Impregnation vs. coprecipitation. Appl Catal A Gen 423-424:42–51. https://doi.org/10.1016/j.apcata.2012.02.017

Yu ZY, Fan XH, Gan M, Chen XL, Lv W (2017) NOx reduction in the iron ore sintering process with flue gas recirculation. JOM 69:1570–1574. https://doi.org/10.1007/s11837-017-2268-z

Zhang HY, Zhu AM, Wang XK, Wang Y, Shi C (2007a) Catalytic performance of Ag–Co/CeO2 catalyst in NO–CO and NO–CO–O2 system. Catal Commun 8:612–618. https://doi.org/10.1016/j.catcom.2006.08.012

Zhang LL, Yao XJ, Lu YY, Sun CZ, Tang CJ, Gao F, Dong L (2018a) Effect of precursors on the structure and activity of CuO-CoOx/gamma-Al2O3 catalysts for NO reduction by CO. J Colloid Interface Sci 509:334–345. https://doi.org/10.1016/j.jcis.2017.09.031

Zhang X, Cheng X, Ma C, Wang X, Wang Z (2018b) Effect of a ZrO2 support on Cu/Fe2O3–CeO2/ZrO2 catalysts for NO removal by CO using a rotary reactor. Catalysis Sci Tech 8:5623–5631. https://doi.org/10.1039/c8cy01546e

Zhang XX et al (2017a) Mechanistic insight into nanoarchitected Ag/Pr6O11 catalysts for efficient CO oxidation. Ind Eng Chem Res 56:11042–11048. https://doi.org/10.1021/acs.iecr.7b02530

Zhang XY, Cheng XX, Ma CY, Wang ZQ (2018c) Effects of the Fe/Ce ratio on the activity of CuO/CeO2–Fe2O3 catalysts for NO reduction by CO. Catalysis Sci Tech 8:3336–3345. https://doi.org/10.1039/c8cy00709h

Zhang XY, Ma CY, Cheng XX, Wang ZQ (2017b) Performance of Fe-Ba/ZSM-5 catalysts in NO + O 2 adsorption and NO + CO reduction. Int J Hydrog Energy 42:7077–7088. https://doi.org/10.1016/j.ijhydene.2017.01.067

Zhang Y, Wang XD, Zhu YY, Zhang T (2013) Stabilization mechanism and crystallographic sites of Ru in Fe-promoted barium hexaaluminate under high-temperature condition for N2O decomposition. Appl Catal B Environ 129:382–393. https://doi.org/10.1016/j.apcatb.2012.10.001

Zhang YB, Liu BB, Su ZJ, Li GH, Fan ZY, Jiang T (2014) Effect of CO and CO2 content in suction gas on sintering process for iron ores. ISIJ Int 54:1991–1993. https://doi.org/10.2355/isijinternational.54.1991

Zhang YP, Fei JH, Yu YM, Zheng XM (2007b) Study of CO2 hydrogenation to methanol over Cu-V/γ-Al2O3 catalyst. J Nat Gas Chem 16:12–15. https://doi.org/10.1016/s1003-9953(07)60019-x

Zhang ZL, Yang XY (2003) Separate/simultaneous catalytic reduction of sulfur dioxide and/or nitric oxide by carbon monoxide over TiO2-promoted cobalt sulfides. J Mol Catal A Chem 195:189–200. https://doi.org/10.1016/s1381-1169(02)00548-4